Toxicology and Applied Pharmacology 289 (2015) 442–456

Contents lists available at ScienceDirect

Toxicology and Applied Pharmacology

journal homepage: www.elsevier.com/locate/ytaap

Development of a physiologically based pharmacokinetic model for assessment of human exposure to bisphenol A

Xiaoxia Yang [a,*], Daniel R. Doerge [a], Justin G. Teeguarden [b,c], Jeffrey W. Fisher [a]

[a] Division of Biochemical Toxicology, National Center for Toxicological Research, U.S. Food and Drug Administration, Jefferson, AR 72079, United States
[b] Health Effects and Exposure Science, Pacific Northwest National Laboratory, Richland, WA 99352, United States
[c] Department of Environmental and Molecular Toxicology, Oregon State University, Corvallis, OR 97331, United States

ARTICLE INFO

Article history:
Received 3 September 2015
Revised 20 October 2015
Accepted 27 October 2015
Available online 29 October 2015

Keywords:
Bisphenol A
BPA
Physiologically based pharmacokinetic model
PBPK
Human

ABSTRACT

A previously developed physiologically based pharmacokinetic (PBPK) model for bisphenol A (BPA) in adult rhesus monkeys was modified to characterize the pharmacokinetics of BPA and its phase II conjugates in adult humans following oral ingestion. Coupled with in vitro studies on BPA metabolism in the liver and the small intestine, the PBPK model was parameterized using oral pharmacokinetic data with deuterated-BPA (d_6-BPA) delivered in cookies to adult humans after overnight fasting. The availability of the serum concentration time course of unconjugated d_6-BPA offered direct empirical evidence for the calibration of BPA model parameters. The recalibrated PBPK adult human model for BPA was then evaluated against published human pharmacokinetic studies with BPA. A hypothesis of decreased oral uptake was needed to account for the reduced peak levels observed in adult humans, where d_6-BPA was delivered in soup and food was provided prior to BPA ingestion, suggesting the potential impact of dosing vehicles and/or fasting on BPA disposition. With the incorporation of Monte Carlo analysis, the recalibrated adult human model was used to address the inter-individual variability in the internal dose metrics of BPA for the U.S. general population. Model-predicted peak BPA serum levels were in the range of pM, with 95% of human variability falling within an order of magnitude. This recalibrated PBPK model for BPA in adult humans provides a scientific basis for assessing human exposure to BPA that can serve to minimize uncertainties incurred during extrapolations across doses and species.

Published by Elsevier Inc.

1. Introduction

Bisphenol A (BPA), a high-production-volume industrial chemical used as a monomer in the production of polycarbonate plastics and epoxy resins, is present in a variety of consumer products, such as food containers and medical devices (EFSA, 2014; FDA, 2014a; Willhite et al., 2008). In the U.S., more than 90% of the population has detectable levels of BPA in their urine (Calafat et al., 2008), suggesting that human exposure to BPA is widespread. The primary route of human exposure to BPA is through the diet, with marginal contributions from non-food sources (Geens et al., 2012; WHO, 2011; EFSA, 2014). Currently, the dietary intake of BPA, estimated by the U.S. Food and Drug Administration (FDA), is 0.2–0.5 μg/kg body weight (BW)/day (mean-90th percentile) for the U.S. population aged 2 years and older (FDA, 2014b).

In vivo and in vitro studies have been conducted to investigate the metabolism and disposition of BPA in humans (Coughlin et al., 2012; Kuester and Sipes, 2007; Kurebayashi et al., 2010; Mazur et al., 2010; Trdan Lusin et al., 2012; Volkel et al., 2005; Völkel et al., 2002). After oral administration of BPA in a hard gelatin capsule, BPA was rapidly and completely absorbed (Volkel et al., 2005; Völkel et al., 2002). The primary metabolic pathway for BPA in the liver is via phase II conjugation, yielding an extensive production of BPA glucuronide (BPAG) and a small amount of BPA sulfate (BPAS) (Kurebayashi et al., 2010). In addition, glucuronidation of BPA in the human small intestine has been characterized (Mazur et al., 2010; Trdan Lusin et al., 2012). Because of extensive first-pass metabolism, serum levels of unconjugated BPA following oral ingestion are very low, leading to undetectable levels in the original human study (Völkel et al., 2002). Urinary excretion of the conjugated BPA is the predominant elimination route for BPA in humans (Teeguarden et al., 2011; Teeguarden et al., 2015; Thayer et al., 2015; Volkel et al., 2005; Völkel et al., 2002).

Due to the ubiquitous nature of BPA, the potential effects associated with BPA exposure, along with some unusually high serum levels of BPA reported in humans, have been the focus of debate surrounding BPA safety (LaKind et al., 2012; Lang et al., 2008; Melzer et al., 2010; Silver et al., 2011; Teeguarden et al., 2013; Teeguarden et al., 2011). One important element to better address and help resolve these controversies is to characterize the processes underlying the pharmacokinetic behavior of BPA in humans. Physiologically based pharmacokinetic (PBPK) modeling, with the integration of physiological and biochemical information into a mechanistic framework, has been commonly used in

* Corresponding author at: U.S. Food & Drug Administration, National Center for Toxicological Research, 3900 NCTR Road, Jefferson, AR 72079, United States.
E-mail address: xiaoxia.yang@fda.hhs.gov (X. Yang).

http://dx.doi.org/10.1016/j.taap.2015.10.016
0041-008X/Published by Elsevier Inc.

human health risk assessment to describe quantitatively the pharmacokinetics of chemicals and their metabolites in humans.

Several PBPK models have been developed to characterize the pharmacokinetics of BPA in humans following oral exposure (Edginton and Ritter, 2009; Fisher et al., 2011; Mielke and Gundert-Remy, 2009, 2012; Partosch et al., 2013; Teeguarden et al., 2005). However, because of the lack of adequately sensitive analytical methods for unconjugated BPA, no kinetic data sets were available in humans to inform the time course for serum (plasma) BPA concentrations. The initial data set (Völkel et al., 2002) used for model calibration only reported serum concentration and urinary excretion time profiles for BPAG, but not for unconjugated BPA. Therefore, model parameters for unconjugated BPA, the active parent compound, in existing human PBPK models, e.g. BPA metabolic constants, could not be directly calibrated based upon available human kinetic data. Considerable efforts have been made to address this issue. For example, in the human PBPK model developed by Edginton and Ritter (2009), systemic clearance of BPA was set to the lower bound needed to maintain serum unconjugated BPA levels below the limit of detection (10 nM) in the human study (Völkel et al., 2002). This is a conservative estimate and represented the "worst-case scenario" as the authors noted (Edginton and Ritter, 2009). Fisher et al. (2011) and Teeguarden et al. (2005) estimated internal dose levels of BPA in humans by scaling of model parameters calibrated against available pharmacokinetic data collected in experimental animals (monkeys and rats) to humans. In addition, an in-vitro-to-in-vivo extrapolation (IVIVE) approach has been applied to derive BPA metabolic constants from in vitro metabolism data (Mielke and Gundert-Remy, 2009, 2012; Partosch et al., 2013). Despite these efforts, because of the lack of justification using kinetic data where the time course of serum BPA concentrations is available, there exists uncertainty in the calibration of BPA model parameters, e.g. parameters describing the oral uptake of BPA and metabolism of BPA in the liver and the small intestine.

In the current paper, the previously developed monkey BPA PBPK model by Fisher et al. (2011) is modified to describe the pharmacokinetic behavior of orally derived BPA in humans, and used to assess human exposure to BPA. The newly collected human kinetic data sets (Teeguarden et al., 2015; Thayer et al., 2015) used for model development characterized for the first time serum concentration and urinary excretion profiles of deuterated-BPA (d_6-BPA) and its phase II conjugates d_6-BPAG and d_6-BPAS in adult humans following a single oral dose of d_6-BPA. The capability to quantify unconjugated BPA in human biological specimens without background interference offers direct empirical evidence for the estimation of BPA model parameters, i.e. parameters describing the oral uptake of BPA and BPA conjugation in the liver and the small intestine. Also, the quantification of individual BPAG and BPAS concentrations, instead of BPAG alone or total BPA conjugates, provides more specific information on the description of BPA detoxification via glucuronidation and sulfation in a quantitative manner. Monte Carlo analyses were then incorporated into the recalibrated PBPK model to address inter-individual kinetic variability, and to assess the distribution of BPA internal dose metrics relevant to the estimated daily BPA intake derived from food ingestion (FDA, 2014b) and the urinary biomonitoring data (Lakind and Naiman, 2008).

2. Materials and methods

2.1. Key pharmacokinetic studies

The data sets used for model calibration were taken from a recent clinical study, in which six adult men and eight adult women were given a single oral dose of 100 μg/kg d_6-BPA via a vanilla wafer cookie after overnight fasting (referred to as cookie data) (Thayer et al., 2015). The use of stable isotope labeled BPA circumvented potential contamination from the laboratory environment and BPA-containing materials encountered during sampling and analysis. After dosing, blood samples (total 29 time points) were collected over a period of 72 h and serum was separated. In addition, all urine specimens voided during the course of blood collections were also collected, for which the time and the volume of each micturition were recorded. Concentrations of d_6-BPA, d_6-BPAG, and d_6-BPAS in serum and urine were determined for each individual using LC–MS/MS methods (Churchwell et al., 2014; Doerge et al., 2011; Twaddle et al., 2010). The cumulative urinary excretion was calculated as the sum of the products of the concentration in each voided sample and the corresponding voided volume. In three subjects (1 male and 2 females), urinary excretion over a period of three days was extremely low (less 55% of the administered dose). Therefore, a separate round of dosing was performed for these three subjects where only serial urine specimens were collected, from which it was determined that essentially quantitative excretion had also occurred (Thayer et al., 2015). The time courses of serum concentration and urinary excretion profiles collected from the other 11 subjects (5 males and 6 females) during the first round of dosing were used for model calibration.

The second round of urinary excretion data, along with the serum concentration profiles collected from the first round of dosing, in these three subjects, 1 male and 2 females (Thayer et al., 2015), were used for model evaluation. In addition, another three pharmacokinetic studies with BPA in adult humans were used for model evaluation. In the first study (Völkel et al., 2002), the time courses of plasma concentration and urinary excretion of deuterated-BPA (d_{14}-BPA) and d_{14}-BPAG were evaluated in adult humans, three female subjects (A, B, C) and three male subjects (E, F, G), after a single oral dosing of 5 mg d_{16}-BPA in a hard gelatin capsule. Plasma samples were collected at 4-h intervals over 32 h for the measurement of d_{14}-BPA and d_{14}-BPAG concentrations, and urine samples were collected at 6-h intervals over 42 h for the analysis of urinary excretion of d_{14}-BPA and d_{14}-BPAG. In the second part of the study, an additional three male subjects (M, N, O) together with the male subject G were dosed orally with 5 mg d_{16}-BPA and plasma samples (8 time points) were collected over 6 h for the measurement of d_{14}-BPA and d_{14}-BPAG concentrations.

An LC–MS/MS method was employed for the measurement of d_{14}-BPA and d_{14}-BPAG concentrations in plasma and urine. Levels of d_{14}-BPA were always below the limit of detection in both plasma (10 nM) and urine (6 nM) samples for all subjects, and only d_{14}-BPAG concentrations were measurable. Individual data for urinary excretion of d_{14}-BPAG in 6 subjects (A, B, C, E, F, and G) and the time course of plasma concentrations of d_{14}-BPAG in subjects M, N, O, and G were kindly provided by Drs. Völkel, Dekant and Popa-Henning (Fisher et al., 2011).

Another data set used for model evaluation was from Volkel et al. (2005), in which the kinetics of urinary excretion from adult humans exposed to BPA was investigated using an HPLC–MS/MS method. Background BPA in blanks or injected solvents was reduced to below the limit of detection (2.5 pmol/ml) using the optimized gradient method. Six subjects, three men and three women, were given a single oral dose of BPA (25 μg/person) in 50 ml of water. Urine specimens were collected at defined intervals (four time points) over a period of 7 h after dosing and voided volumes were recorded. Concentrations of BPA in most samples were below the limit of detection (2.5 pmol/ml) and only the kinetics of excretion with urine of BPAG and total BPA after glucuronidase treatment were reported (Volkel et al., 2005).

The final data set used for model evaluation was from a recent pharmacokinetic study (Teeguarden et al., 2015), where measurements of unconjugated d_6-BPA and its phase II metabolites (d_6-BPAG and d_6-BPAS) in serum and urine were carried out in ten adult men following a single oral dosing of 30 μg/kg of d_6-BPA delivered in a commercial tomato soup (referred to as soup data). Volunteers were not required to fast overnight and breakfast was provided before BPA ingestion. Blood samples were drawn at defined intervals over a 24 h period (16 time points) after ingesting the soup. The average period of time for soup ingestion was 9.2 min. Voided urine was collected at intervals corresponding to the timing of blood draws over a period of 13 h and then

as volunteered at time points up to 24 h after ingestion, with voided volumes recorded. Concentrations of unconjugated d_6-BPA (Patterson et al., 2013), d_6-BPAG, and d_6-BPAS (Churchwell et al., 2014) in serum, as well as total d_6-BPA (Twaddle et al., 2010) in urine, were measured. The accumulated urinary excretion was obtained as the sum of the products of the concentration in each voided sample and the corresponding voided volume. The time courses of serum concentrations of d_6-BPA, d_6-BPAG, and d_6-BPAS, together with the cumulative excretion of total d_6-BPA in the urine, were used for model evaluation.

2.2. PBPK model for BPA and its phase II metabolites

An eight-compartment PBPK model for BPA (serum, liver, fat, gonads, richly perfused tissues, slowly perfused tissues, brain, and skin) and two single-compartment (volume of distribution, Vbody) submodels for BPAG and BPAS were constructed (Fig. 1). In accordance with the original model (Fisher et al., 2011), the selection of compartments was based on kinetic considerations (e.g. liver) and the model's potential use for internal dose metrics estimation (e.g. brain and gonads). Different from the original model, a skin compartment was introduced for the future assessment of dermal exposure, considering that exposure to BPA via the skin may be of interest for certain subpopulations such as cashiers (Biedermann et al., 2010; Zalko et al., 2011). The phase II metabolites, BPAG and BPAS, were simply described as a single non-physiological compartment given that these conjugates display no known estrogenic activity (Matthews et al., 2001; Shimizu et al., 2002). Ten percent of BPAG derived from the small intestine and the liver was assumed to be secreted into the gut through the bile ducts, and undergo enterohepatic recirculation (EHR) as assumed previously by Teeguarden et al. (2005), whereas the remaining 90% of BPAG formed was taken up into the volume of the distribution (systemic circulation) in the BPAG sub-model. Such an assumption is critical to describe the lingering of serum d_6-BPAG levels, as well as serum d_6-BPA levels, at later time points. With no information to assume otherwise, BPA sulfation was assumed to occur only in the liver and the resulting BPAS was taken up completely into the systemic circulation. No biliary excretion of BPAS was assumed to occur.

The physiological model parameters for adult humans were taken from the published literature or set to the study-specific values (Table 1), with the exception of the percent body fat (VFatC), which was estimated using a linear regression equation as a function of age and natural log transformed body mass index (BMI) (Jackson et al., 2002). BMI was calculated as weight in kilograms divided by height in meters squared.

$$\mathrm{VFatC\,(female)} = (-102.01 + 39.96 \times \ln \mathrm{BMI} + 0.14 \times \mathrm{age})/100 \quad (1a)$$

$$\mathrm{VFatC\,(male)} = (-103.94 + 37.31 \times \ln \mathrm{BMI} + 0.14 \times \mathrm{age})/100 \quad (1b)$$

Tissue-to-serum distribution ratios for BPA used in the original model (Fisher et al., 2011) were used in this study (Table 2). For skin, the partition coefficient was adopted from (Mielke et al., 2011), where it was calculated using the algorithm developed by Schmitt (Schmitt, 2008).

Coding and simulations were performed using the acslX program, version 3.0.2.1 (The Aegis Technologies Group, Inc., Huntsville, Alabama). Model code is provided in the Supplementary data section and m files containing data and plot commands are available upon request.

2.3. Model development

2.3.1. BPA: hepatic metabolism. Based upon in vitro metabolism studies of BPA in the liver, an IVIVE approach was employed to derive model parameters representing hepatic glucuronidation and sulfation of BPA, which were described using Michaelis–Menten equations. The Michaelis constant (Kmliver, nM) for hepatic BPA glucuronidation was set equal to the reported Km value of 45,800 nM, experimentally determined using pooled male and female human liver microsomes (Coughlin et al., 2012) (Table 3). The maximum reaction velocity for hepatic glucuronidation (VmaxliverC) was derived from a reported in vitro maximal velocity of 4.71 nmol/min/mg protein (Coughlin et al., 2012), by accounting for microsomal protein content of the human liver (32 mg microsomal protein/g liver) (Barter et al., 2007) and model predicted liver weight (2.132 kg, for a man with body weight of 82 kg). No sex

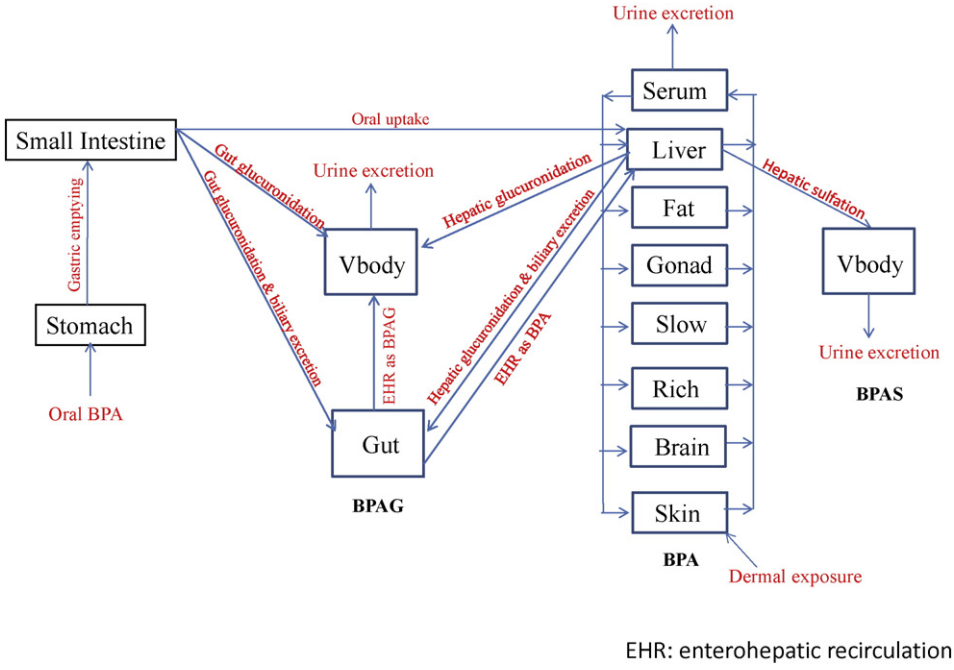

Fig. 1. Schematic depicting the adult human PBPK model for bisphenol A (BPA) and its phase II metabolites, BPA glucuronide (BPAG) and BPA sulfate (BPAS). Orally administered BPA is subject to presystemic metabolism in the liver and the small intestine, resulting in the formation of BPAG and BPAS. The majority of BPAG in the liver derived from the small intestine and the liver (MET, 90%) is directly taken up into the volume of distribution in the BPAG sub-model, with a small portion (10%) secreted into the small intestine via the bile ducts and undergoes subsequent enterohepatic recirculation (EHR).

Table 1
Physiological model parameters.

Parameters	Values	References
Body weight, BW (kg)	Study specific	Experimental data
Cardiac output, QCC (L/h/kg$^{0.75}$)	15.87	Fisher et al. (2011))
Blood flows (fraction of cardiac output)		
Fat (QFatC)	0.053/0.091[a]	Edginton et al. (2006)
Liver (QLiverC)	0.24	Fisher et al. (2011)
Brain (QBrainC)	0.11	Brown et al. (1997)
Skin (QSkinC)	0.058	Brown et al. (1997)
Gonads (QGonadC)	0.00054/0.00022[a]	Edginton et al. (2006)
Richly perfused (QRC)	0.76 − QLiverC − QBrainC	
Slowly perfused (QSC)	0.24 − QFatC − QGonadC − QSkinC	
Tissue volumes (fraction of body weight)		
Plasma (VPlasmaC)	0.0435	Fisher et al. (2011)
Fat (VFatC)	Calculated	Jackson et al. (2002)
Liver (VLiverC)	0.026	Brown et al. (1997)
Brain (VBrainC)	0.02	Brown et al. (1997)
Skin (VSkinC)	0.0371	Brown et al. (1997)
Gonads (VGonadC)	0.0007/0.0027[a]	Fisher et al. (2011)
Richly perfused (VRC)	0.33 − VLiverC − VBrainC	
Slowly perfused (VSC)	0.60 − VFatC − VSkinC − VGonadC	

[a] Male/female.

difference was observed in the glucuronidation of BPA in human liver microsomes (Elsby et al., 2001). The fraction unbound in the microsomes was not accounted for in the calculation of the in vivo values.

To describe the sulfation of BPA in the liver, the Michaelis constant (Kmlivers, nM) was set to the reported Km value of 10,100 nM, experimentally determined using cryopreserved hepatocytes of humans (Kurebayashi et al., 2010). The maximum reaction velocity for hepatic sulfation (VmaxliversC) was derived from a reported in vitro maximal velocity of 149 nmol/h/g liver (Kurebayashi et al., 2010), by accounting for model predicted liver weight (2.132 kg, for a man with body weight of 82 kg).

2.3.2. BPA: oral uptake and gastrointestinal (GI) tract metabolism. After oral administration, gastric emptying of BPA into the small intestine was described using a first order gastric emptying constant (GEC, L/h/kg$^{-0.25}$) set to a value of 3.5 L/h/kg$^{-0.25}$ (Fisher et al., 2011; Kortejarvi et al., 2007). BPA emptied from the stomach lumen into the small intestine lumen was assumed to be immediately available within enterocytes by passive diffusion, where BPA is either rapidly absorbed into the portal blood supply (Völkel et al., 2002) or subject to glucuronidation in the GI tract (Trdan Lusin et al., 2012), as described in the original monkey BPA PBPK model (Fisher et al., 2011).

Table 2
Estimated tissue-serum distribution coefficients for BPA. Tissue-serum distribution coefficients for BPA were set to in vivo tissue-serum distribution ratios obtained in adult rats (Fisher et al., 2011), with exception of the skin (Mielke et al., 2011).

Tissues	Partition coefficients (tissue/serum)
Fat (Pfat)	5.0
Brain (Pbrain)	2.8
Richly perfused tissues (set to brain) (Prich)	2.8
Slowly perfused tissues (set to muscle) (Pslow)	2.7
Gonads (Pgonads)	2.6
Skin (Pskin)	5.7
Liver (Pliver)	0.73

Table 3
Chemical specific model parameters.

Parameters	Values	References
BPA		
Hepatic glucuronidation		
Kmliver (nM)	45,800	Coughlin et al. (2012)
VmaxliverC (nmol/h/kg$^{0.75}$)	707,537	Coughlin et al. (2012)
Hepatic sulfation		
Kmlivers (nM)	10,100	Kurebayashi et al. (2010)
VmaxliversC (nmol/h/kg$^{0.75}$)	11,657	Kurebayashi et al. (2010)
Gastric emptying (GEC, L/h/kg$^{-0.25}$)	3.5	Fisher et al. (2011), Kortejarvi et al. (2007)
Oral uptake, from small intestine to liver (K1C, L/h/kg$^{-0.25}$)	2[a]	Optimize
Glucuronidation in enterocytes		
KmgutC (nM)	58,400	Trdan Lusin et al. (2012)
VmaxgutC (nmol/h/kg$^{0.75}$)	22,750	Trdan Lusin et al. (2012)
Urinary excretion (KurinebpaC, L/h/kg$^{0.75}$)	0.06	Optimize
BPAG		
Uptake from enterocytes into the liver (KGlinC, L/h/kg$^{-0.25}$)	50	Visual fit
Volume of distribution (VbodyC, fraction of body weight)	0.0435	Set to plasma volume (Fisher et al., 2011)
Fraction of BPAG in the liver delivered to systemic circulation (MET)	0.9	Teeguarden et al. (2005)
Urinary excretion (KurineC, L/h/kg$^{0.75}$)	0.35	Optimize
Enterohepatic recirculation (EHR)		
EHR as BPA (Kenterobpa1C, L/h/kg$^{-0.25}$)	0.2	Visual fit
EHR as BPAG (EHRrateC, L/h/kg$^{-0.25}$)	0.2	Visual fit
BPAS		
Volume of distribution (VbodysC, fraction of body weight)	0.0435	Set to plasma volume (Fisher et al., 2011)
Urinary excretion (KurinebpasC, L/h/kg$^{0.75}$)	0.03	Optimize

[a] A decreased K1C value of 0.51 L/h/kg$^{-0.25}$ is needed when BPA is delivered in commercial tomato soup (Teeguarden et al., 2015).

The oral uptake of BPA from enterocytes into the portal blood supply and the liver was described as a first order process (K1C, L/h/kg$^{-0.25}$), obtained by visual fitting and optimization to achieve agreement with serum concentration profiles of d_6-BPA in adult humans orally dosed with 100 μg/kg of d_6-BPA (Thayer et al., 2015). Optimization was conducted using the Levenberg–Marquardt algorithm in all cases. To ensure the robustness, consistent convergence of parameter values was tested with starting values of K1C varied from one-half to 2 times the starting value.

Phase II metabolism of BPA via glucuronidation in the GI tract was described using a Michaelis–Menten equation. For which, the Michaelis constant (KmgutC, nM) was set equal to a value of 58,400 nM, determined using human intestinal microsomes (Trdan Lusin et al., 2012). The maximum reaction velocity (VmaxgutC) was derived from in vitro maximal velocity of 1.4 nmol/min/mg protein to account for microsomal protein content of the human intestine (3 mg/g tissue) and the weight of the human intestine (30 g/kg body weight) (Trdan Lusin et al., 2012). With no information to assume otherwise, glucuronidation of BPA was expected to occur within enterocytes located in various regions of the small intestine (duodenum, jejunum and ileum). Therefore, the sum of regional weights (volumes) of the enterocytes in the duodenum (18.2 g), jejunum (65.8 g), and ileum (38.3 g) (Paine et al., 1997; Yu et al., 1996) was considered as the volume of BPA distribution in the small intestine and used for the calculation of BPA concentration in the small intestine.

2.3.3. BPA: urinary excretion. Small amounts of unconjugated d_6-BPA (<0.1% of administered dose) were detected in the urine of adult humans orally dosed with d_6-BPA (Teeguarden et al., 2015; Thayer

et al., 2015). As such, excretion of BPA into the urine was introduced to the current model. Urinary excretion of BPA was described using a clearance term from blood (KurinebpaC, L/h/kg$^{0.75}$), which was determined by visual fitting and optimization using the Levenberg–Marquardt algorithm to achieve agreement with serum concentration and urinary excretion profiles of d_6-BPA in adult humans after a single oral dose of 100 μg/kg d_6-BPA (Thayer et al., 2015).

BPA concentration (ConurineBPA, nM) in each voided urine was simulated as

$$\text{ConurineBPA} = A_{\text{urineBPA}}/V_{\text{urine}} \quad (2)$$

where A_{urineBPA} (nmol) is model simulated amount of BPA accumulated in the bladder over the time between the current void and the previous void, and V_{urine} (L) is the measured volume of the urine for the current void (Bartels et al., 2012).

2.3.4. BPAG: formation, distribution and systemic circulation. The rate of BPAG formation equals to the rate of BPA glucuronidation in the liver and the small intestine (Fisher et al., 2011). Consistent with the previous assumption (Teeguarden et al., 2005), ninety percent (MET) of the resulting BPAG in the liver derived from glucuronidation in the small intestine and the liver was assumed to be taken up immediately into the systemic circulation (volume of distribution, VbodyC), whereas the remaining ten percent was assumed to be secreted into the gastrointestinal tract (GI tract) via the bile duct (see below for details).

Uptake of BPAG produced in the small intestine to the liver via the portal vein was described using a first order term (KGIinC, L/h/kg$^{-0.25}$), obtained by visual fitting to the time course of serum d_6-BPAG concentration in adult humans orally dosed with 100 μg/kg d6-BPA (Thayer et al., 2015). Optimization using the Levenberg–Marquardt algorithm was attempted, but failed to converge. Therefore, the visually fitted KGIinC value was used.

Given that BPAG is highly soluble in water (Melzer et al., 2010), the volume of distribution (VbodyC, L/kg) for BPAG was initially set to the value of total body water volume (0.6 L/kg) in adult humans (Davies and Morris, 1993) and then reduced to better predict serum d_6-BPAG concentrations in adult humans orally dosed with 100 μg/kg d_6-BPA (Thayer et al., 2015). An optimized VbodyC value of 0.025 L/kg, using the Levenberg–Marquardt algorithm, was then set equal to the plasma volume (0.0435 L/kg) for adult humans.

Excretion of BPAG from the systemic circulation into urine was described using an optimized systemic clearance term (KurineC, L/h/kg$^{0.75}$), obtained by simultaneous fitting to the time course of serum d_6-BPAG concentration and cumulated urinary excretion profiles of d_6-BPAG after oral dosing of 100 μg/kg of d_6-BPA in adult humans (Thayer et al., 2015). Optimization was carried out using the Levenberg–Marquardt algorithm.

Ten percent of BPAG in the liver derived from glucuronidation in the liver and the small intestine were assumed to be secreted into the GI tract via the bile duct. The resulting d_6-BPAG in the terminal region of the small intestine was assumed to undergo deconjugation through the action of bacterial β-glucuronidase in the small intestine, resulting in the formation of unconjugated BPA, which was either reabsorbed into the liver via portal vein (EHR for BPA, Kenterobpa1C, L/h/kg$^{-0.25}$), or converted to BPAG within enterocytes and then reabsorbed into the systemic circulation (EHR for BPAG, EHRrateC, L/h/kg$^{-0.25}$) as described previously (Yang et al., 2013). In accordance with the previous rat model (Yang et al., 2013), these processes were grouped and simply described using "non-physiological composite" first order terms. The values of Kenterobpa1C and EHRrateC were determined by visual fitting to serum d_6-BPAG and d_6-BPA concentration profiles in adult humans orally administered with 100 μg/kg d_6-BPA (Thayer et al., 2015). Optimization was conducted using the Levenberg–Marquardt algorithm, but no successful convergence was achieved.

2.3.5. BPAS: formation, distribution and systemic circulation. The formation of BPAS was assumed to occur in the liver (Kurebayashi et al., 2010), but not in the small intestine due to the lack of direct empirical evidence. In accordance with BPAG, the volume of distribution (VbodyC, L/kg) for BPAS was set equal to the value of plasma volume (0.0435 L/kg) in adult humans (Fisher et al., 2011). Systemic clearance term for BPAS (KurinebpasC, L/h/kg$^{0.75}$) was obtained by visual fitting and optimization using the Levenberg–Marquardt algorithm to achieve agreement with the time course of serum d_6-BPAS concentration and cumulated urinary excretion profiles of d_6-BPAS after oral administration of 100 μg/kg d_6-BPA in adult humans (Thayer et al., 2015).

2.4. Assessment of model performance

To assess model performance, the mean relative deviation (MRD) and the average fold error (AFE) were calculated to provide a measurement of prediction precision and bias with equal value to under- and over-predictions, using Eqs. (3) and (4), respectively (Edginton et al., 2006; Ito and Houston, 2005; Riley et al., 2005; Vogt, 2014).

$$\text{MRD} = 10^{\sqrt{\frac{\sum_{i=1}^{n}(\log(\text{predicted}) - \log(\text{observed}))^2}{n}}} \quad (3)$$

$$\text{AFE} = 10^{\left|\frac{\sum_{i=1}^{n}(\log(\text{predicted}) - \log(\text{observed}))}{n}\right|} \quad (4)$$

where predicted is the model predicted value, observed is the reported value, and N represents the number of observations. These figures of merits (ARD and AFE) were calculated for the time course of serum concentrations and the amount excreted in each voided urine, but not the cumulative amount to avoid the bias because of accumulation.

2.5. Sensitivity analysis

A local sensitivity analysis was implemented using the built-in functionality of acsIX to assess the impact of model parameter perturbations on the model output, i.e. model predicted serum BPA concentrations, as a function of time. A single oral dose of 100 μg/kg of d_6-BPA was simulated for adult humans. The normalized sensitivity coefficient (NSC) was calculated by the following equation (Clewell et al., 1994):

$$\text{NSC} = \frac{(O_i - O)/O}{(P_i - P)/P} \quad (5)$$

where O is the model output resulting from the original parameter value, O_i is the model output resulting from the 1% increase in the parameter value, P is the original parameter value, and P_i is the parameter value increased by 1%. A positive NSC suggests a direct correlation between the model output and the corresponding parameter, while a negative NSC indicates the model output is inversely associated with the specific parameter. Parameters with maximum absolute NSC values over a 24 h period exceeding 0.1 were considered to be sensitive. A NSC value of 1 indicates that the changes in the model parameter and the model output display a 1 to 1 relationship. Those parameters with maximum absolute NSC values greater than 1 were considered to have a high impact on model output.

2.6. Monte Carlo analysis

Monte Carlo simulations were implemented to evaluate the impact of uncertainty and inter-individual variability on human BPA pharmacokinetics. Normal distribution of model parameters was assumed for blood flows and tissue volumes; while cardiac output, partition coefficients, and chemical specific model parameters were assumed to be log-normally distributed (Clewell et al., 2000; Shankaran et al., 2013; Sterner et al., 2013; Tan et al., 2006) (Table 4). Model parameters are randomly varied around the values (central tendencies) established during model calibration. Probabilistic distributions (variability) of model parameter values are derived from previous reported inter-individual variability (Clewell et al., 2000; Delic et al., 2000; Shankaran et al., 2013; Tan et al., 2006). Of which, the coefficients of variation (CV, the ratio of standard deviation to mean) of 9% and 20% were assumed for cardiac output and partition coefficients, respectively, while a CV of 30% was assumed for the rest model parameters (chemical specific model parameters, blood flows and tissue volumes) unless otherwise specified. The variability for the metabolic constants of hepatic glucuronidation was estimated from reported individual values in the literature (Kuester and Sipes, 2007), with CVs of 36% and 28% for Kmliver and VmaxliverC, respectively. To ensure physiological plausibility, the upper and lower bounds of each distribution, were truncated at 1.96 times the standard deviation (SD) above and below the mean values (95% of distribution). Distributions of body weight for the general adult human population aged 20 years and older were obtained from the National Health and Nutrition Examination Survey (NHANES) III data set (Ogden et al., 2004), and truncated at the 2.5th and 97.5th percentiles as well to comprise 95% of the distribution (Shankaran et al., 2013; Tan et al., 2006). The upper bound of the fraction of BPAG in the liver derived from the small intestine and the liver taken up into the systemic circulation (MET) was set to 1. The model was run 1000 times with model parameters randomly sampled from the defined distributions. To ensure the physiological plausibility of randomly selected physiological parameters, i.e. the sum of the fractional blood flows equals 1 and the sum of the fractional tissue volumes equals 0.93, randomly selected physiological model parameters were adjusted in a fractional manner to maintain mass balance (Covington et al., 2007; Sterner et al., 2013).

Table 4
Parameter distributions used in the Monte Carlo analysis.

Parameters	Mean	SD	Lower bound	Upper bound	Distribution
Blood flows (fraction of cardiac output)					
QCC, L/h/kg$^{0.75}$	15.87	1.4	13.1	18.7	Lognormal
QFatC	0.053	0.016	0.021	0.084	Normal
QLiverC	0.24	0.072	0.099	0.38	Normal
QBrainC	0.11	0.033	0.045	0.17	Normal
QSkinC	0.058	0.017	0.024	0.092	Normal
QGonadC	0.00054	0.00016	0.00022	0.00086	Normal
QRC	0.41[a]	0.123	0.16892	0.65108	Normal
QSC	0.12846[a]	0.039	0.05293	0.20399	Normal
Tissues volumes (fraction of body weight)					
Body weight (BW, kg)	82.3	26.4	30.6	134	Normal
VPlasmaC	0.0435	0.013	0.0179	0.0691	Normal
VFatC	0.21	0.063	0.087	0.33	Normal
VLiverC	0.026	0.008	0.011	0.041	Normal
VBrainC	0.02	0.006	0.008	0.03	Normal
VSkinC	0.0371	0.011	0.0153	0.0589	Normal
VGonadC	0.0007	0.0002	0.0003	0.001	Normal
VRC	0.284[a]	0.085	0.117	0.451	Normal
VSC	0.3492[a]	0.105	0.1439	0.5545	Normal
Partition coefficients for BPA					
Pfat	5.0	1	3.0	6.96	Lognormal
Pbrain	2.8	0.56	1.7	3.9	Lognormal
Prich	2.8	0.56	1.7	3.9	Lognormal
Pslow	2.7	0.54	1.64	3.76	Lognormal
Pgonads	2.6	0.52	1.58	3.62	Lognormal
Pskin	5.7	1.14	3.47	7.93	Lognormal
Pliver	0.73	0.146	0.44	1.02	Lognormal
BPA					
Kmliver (nM)	45,800	13,740	18,870	72,730	Lognormal
VmaxliverC (nmol/h/kg$^{0.75}$)	707,537	212,261	291,505	1,123,569	Lognormal
Kmlivers (nM)	10,100	3030	4161	16,039	Lognormal
VmaxliversC (nmol/h/kg$^{0.75}$)	11,657	3497	4803	18,511	Lognormal
GEC (L/h/kg$^{-0.25}$)	3.5	1.1	1.4	5.6	Lognormal
K1C (L/h/kg$^{-0.25}$)	2	0.6	0.8	3.2	Lognormal
KmgutC (nM)	58,400	17,520	24,061	92,739	Lognormal
VmaxgutC (nmol/h/kg$^{0.75}$)	22,750	6825	9373	36,127	Lognormal
KurinebpaC (L/h/kg$^{0.75}$)	0.06	0.018	0.025	0.095	Lognormal
BPAG					
KGlinC (L/h/kg$^{-0.25}$)	50	15	20.6	79.4	Lognormal
VbodyC (fraction of body weight)	0.0435	0.013	0.0179	0.069	Lognormal
KurineC (L/h/kg$^{0.75}$)	0.35	0.105	0.144	0.556	Lognormal
Kenterobpa1C (L/h/kg$^{-0.25}$)	0.2	0.06	0.08	0.32	Lognormal
EHRrateC (L/h/kg$^{-0.25}$)	0.2	0.06	0.08	0.32	Lognormal

[a] Calculated (please refer to model codes for details).

2.7. Assessment of human exposure to BPA

Coupled with Monte Carlo analysis, the human BPA PBPK model was employed to estimate the inter-individual variability in internal dose metrics (serum peak concentration (C_{max}) and daily area under the concentration–time curve (AUC)) of BPA at steady state for the U.S. general population (men) aged 20 years and older relevant to the following exposure scenarios. The FDA reported an updated estimate of BPA dietary intake of 0.2–0.5 μg/kg/day (mean-90th percentile) for the adult U.S. population aged 2 years and older (FDA, 2014b). Based on the National Health and Nutrition Examination Survey (NHANES) 2003–2004 biomonitoring urine data, the estimated total aggregate daily BPA exposure was 0.05–0.27 μg/kg BW/day (median-95th percentile) for U.S. populations aged 6 years and older (Lakind and Naiman, 2008). The estimated intake values derived from the NHANES 2003–2004 biomonitoring urine data are higher than estimates based on other NHANES survey data (2005–2010) (CDC, 2014). To represent the ingestion of BPA with meals, BPA dosing was simulated as an intermittent process, i.e., at three divided doses over a period of 12 h, whereas for the remaining 12 h no exposure occurred.

3. Results

3.1. Model calibration

Fig. 2A and Fig. 3A show model predicted and observed serum d_6-BPA concentration time courses and cumulative excretion profiles of d_6-BPA in urine in adult humans following a single oral dose of 100 μg/kg d_6-BPA delivered in cookies (Thayer et al., 2015). Glucuronidation of d_6-BPA in the liver was described using a Michaelis–Menten affinity constant (Kmliver) of 45,800 nM and a VmaxliverC value of 707,537 nmol/h/kg$^{0.75}$; whereas for sulfation of d_6-BPA in the liver, the Michaelis–Menten affinity constant (Kmlivers) was set to a value of 10,100 nM with a VmaxliversC value of 11,657 nmol/h/kg$^{0.75}$ (Table 3). In the small intestine, glucuronidation of d_6-BPA was described with a Michaelis–Menten affinity constant (KmgutC) of 58,400 nM and a VmaxgutC value of 22,750 nmol/h/kg$^{0.75}$.

With gastric emptying first order constant (GEC) fixed at a value of 3.5 L/h/kg$^{-0.25}$ (Fisher et al., 2011; Kortejarvi et al., 2007), oral uptake of BPA (K1C) into the portal blood and the liver was set to a value of 2 L/h/kg$^{-0.25}$, obtained by optimization to fit serum d_6-BPA concentrations after oral administration of 100 μg/kg d_6-BPA in adult humans (Thayer et al., 2015). EHR of d_6-BPA (Kenterobpa1C) was set to a

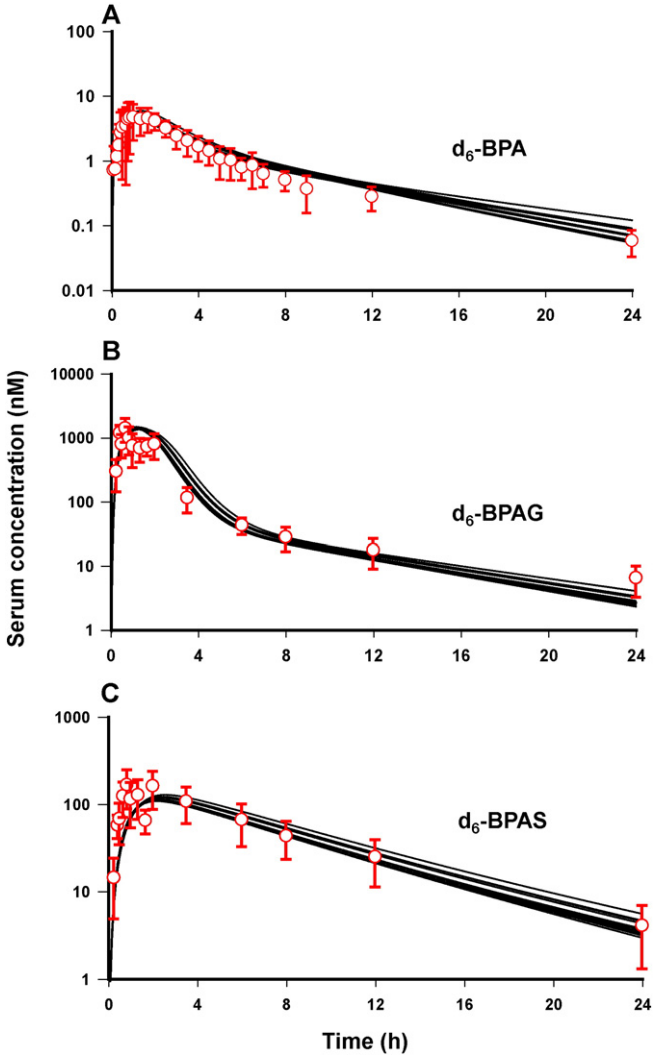

Fig. 2. Concentration–time profiles after oral dosing of adult humans (n = 11) with 100 μg/kg of deuterated BPA (d_6-BPA) (Thayer et al., 2015). A: Simulated individual (solid lines) and observed (mean ± SD) serum d_6-BPA concentrations; B: simulated individual (solid lines) and observed (mean ± SD) serum d_6-BPAG concentrations; C: simulated individual (solid lines) and observed (mean ± SD) serum d_6-BPAS concentrations. Simulations of individual patients were performed using individual body weights while keeping other model parameters constant.

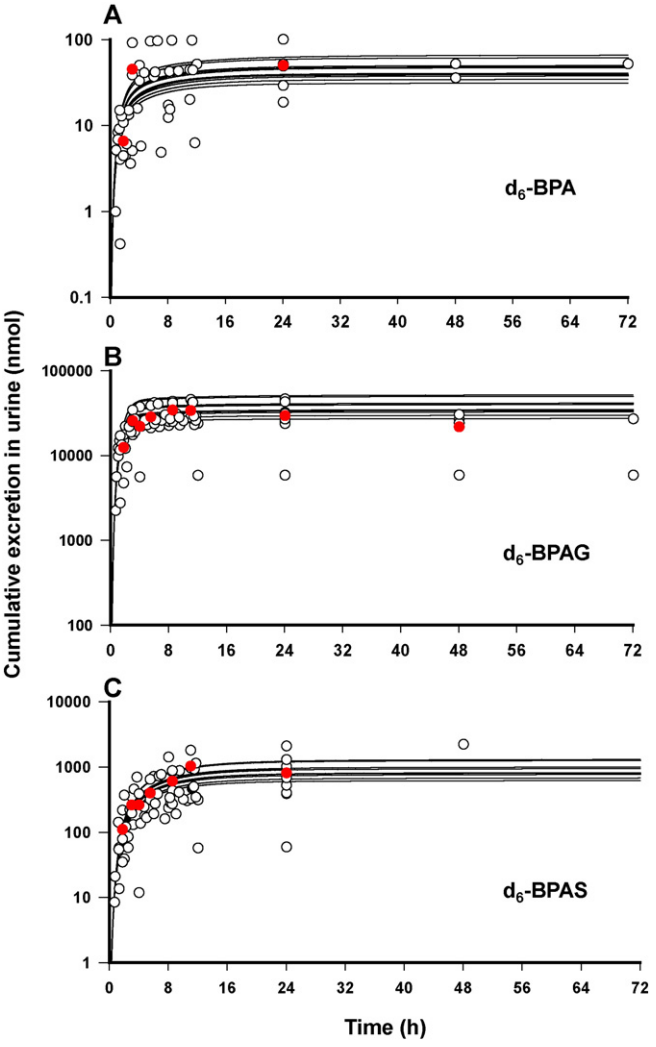

Fig. 3. Urinary excretion profiles after oral dosing of adult humans (n = 11) with 100 μg/kg deuterated BPA (d_6-BPA) (Thayer et al., 2015). A: Simulated individual (solid lines) and observed individual (○) and mean (●) cumulative excretion of d_6-BPA in urine; B: simulated individual (solid lines) and observed individual (○) and mean (●) cumulative excretion of d_6-BPAG in urine; C: simulated individual (solid lines) and observed individual (○) and mean (●) cumulative excretion of d_6-BPAS in urine.

visually fitted first order constant of 0.2 L/h/kg$^{-0.25}$ and systemic excretion of d_6-BPA to urine was described with an optimized clearance term (KurinebpaC) of 0.06 L/h/kg$^{0.75}$ to achieve agreement with time courses of serum d6-BPA concentration and cumulative excretion of d_6-BPA in urine in adult humans (Thayer et al., 2015).

As shown in Fig. 2A, model predicted serum d_6-BPA levels were in excellent agreement with measurements following oral exposure to 100 μg/kg d_6-BPA (Thayer et al., 2015), with MRD ranged from 1.5 to 2.7 (mean, 1.9) and AFE ranged from 1.0–2.5 (mean, 1.5). Results of MRD and AFE values for each simulation are provided in Supplementary data (Table S1). With some exceptions, the model was also capable of tracking cumulative excretion of d_6-BPA into urine following a single oral dose of 100 μg/kg d_6-BPA (Thayer et al., 2015) (Fig. 3A), with average MRD of 6.5 (1.8–31.1) and average AFE of 1.8 (1.0–5.9). The variability in the urinary data is reflected in the range of MRD and AFE values. The model predicted that the majority (approximately 70%) of orally administered d_6-BPA was subject to first-pass metabolism in the small intestine, whereas the remaining (about 30%) was taken up into the portal blood supply, reaching the liver where it was subject to additional first pass metabolism.

Fig. 2B and Fig. 3B show model predicted and observed serum concentration profiles and urinary excretion data of d_6-BPAG in adult humans following a single oral dose of 100 μg/kg d_6-BPA (Thayer et al., 2015). Ten percent of d_6-BPAG arising from the glucuronidation in the liver and the small intestine was assumed to undergo biliary excretion and subsequent enterohepatic recirculation (Teeguarden et al., 2005), with the volume of distribution for d_6-BPAG (VbodyC) fixed to a value of 0.0435 L/kg, corresponding to the volume of plasma in adult humans (Fisher et al., 2011). Systemic clearance of d_6-BPAG into urine (KurineC) was set to an optimized value of 0.35 L/h/kg$^{0.75}$, and EHR of d_6-BPAG was described with a visually fitted first order constant (EHRrateC) value of 0.2 L/h/kg$^{0.75}$, to achieve agreement with serum concentration and cumulative urinary excretion profiles of d_6-BPAG collected in adult humans dosed with 100 μg/kg d_6-BPA (Thayer et al., 2015). As shown in Fig. 2B, model simulated serum d_6-BPAG concentrations were in line with collected kinetic data with MRD of 1.8 (1.5–2.1) and AFE of 1.2 (1.0–1.5). Also, the model in general tracked the kinetic behavior of d_6-BPAG in urine with MRD of 7.8 (1.5–63.3) and AFE of 1.8 (1.1–7.6), except that observations at later time points were somewhat overestimated (Fig. 3B),

Fig. 2C and Fig. 3C show model predicted and observed serum concentration profiles and urinary excretion data of d_6-BPAS in adult

humans following a single oral dose of 100 μg/kg d_6-BPA (Thayer et al., 2015). With the volume of distribution for d_6-BPAS (VbodysC) set to a value of 0.0435 L/kg, corresponding to the volume of plasma in adult humans, systemic clearance of d_6-BPAS into urine was described using an optimized KurinebpasC value of 0.03 L/h/kg$^{0.75}$, obtained by fitting to the collected serum concentration and urinary excretion profiles of d_6-BPAS (Thayer et al., 2015). Simulations of serum d_6-BPAS concentration profiles accurately tracked experimental data, except that at the early time points serum d_6-BPAS concentrations were slightly underestimated [MRD, 2.0 (1.5–3.0); AFE, 1.5 (1.1–1.9)] (Fig. 2C). Model simulated urinary d_6-BPAS kinetic profiles in general agreed with the collected data (Fig. 3C), with MRD of 6.4 (1.3–48.4) and AFE of 1.3 (1.0–1.7).

Model predictions of time courses of serum concentration, cumulative urinary excretion, as well as concentrations of d_6-BPA, d_6-BPAG, and d_6-BPAS in urine for each individual are provided in Supplementary data (Fig. S1).

3.2. Model evaluation

Völkel et al. (2002) reported plasma concentration and urinary excretion-time profiles of d_{14}-BPAG in adult humans after a single oral dosing of 5 mg d_{16}-BPA in a hard gelatin capsule over a period of up to 42 h. The calibrated adult human model adequately reproduced the cumulative excretion of d_{14}-BPAG into urine (Fig. 4A) with MRD of 3.8 (2.8–5.4) and AFE of 2.4 (1.8–2.9). While the model provided a good description of plasma d_{14}-BPAG concentration profiles for the first 4 h, observations at later time points were somewhat underestimated, as shown in Fig. 4B with average MRD of 2.9 (2.0–3.7) and average AFE of 1.4 (1.0–1.5), and in Fig. 4C with average MRD of 4.8 and average AFE of 2.5. Consistent with the original study (Völkel et al., 2002), model predicted serum d_{14}-BPA concentrations were below the limit of detection (10 nM) (Fig. 4C).

Fig. 5 shows model predictions and observations of cumulative excretion of BPAG in urine over a period of 7 h in adult humans following a single oral dose of 25 μg BPA in 50 ml of water (Volkel et al., 2005). The model accurately tracked experimental observations with MRD of 2.7 and AFE of 1.6.

In addition, the concentration time courses in serum, along with urinary excretion profiles, of d_6-BPA and its phase II metabolites, collected from two separate rounds of dosing (100 μg/kg d_6-BPA delivered with cookies) in three subjects (Thayer et al., 2015), were used for model evaluation. Model predicted serum d_6-BPA [MRD, 1.6 (1.5–1.7); AFE, 1.1 (1.0–1.3)] (Fig. 6A), d_6-BPAG [MRD, 1.9 (1.4–2.5); AFE, 1.4 (1.1–2.0)] (Fig. 6B), and d_6-BPAS [MRD, 2.1 (1.5–3.1); AFE, 1.4 (1.1–2.0)] (Fig. 6C) concentration profiles were in excellent agreement with collected data, and the model also tracked the kinetic behaviors of d_6-BPAG [MRD, 2.0 (1.6–2.4); AFE, 1.1 (1.0–1.1)] (Fig. 6D) and d_6-BPAS [MRD, 4.3 (1.8–5.7); AFE, 2.0 (1.1–2.9)] (Fig. 6E) in urine.

Teeguarden et al. (2015) assessed twenty-four hour human serum and urine profiles of d_6-BPA and its phase II metabolites (d_6-BPAG and d_6-BPAS) in adult men over 24 h following a single oral dosing of 30 μg/kg d_6-BPA via a commercial tomato soup. When using the calibrated adult human model based on the cookie data (Thayer et al., 2015), serum d_6-BPA concentrations were over-predicted except for the last time point (Fig. 7A). In attempt to achieve a better fit of serum d_6-BPA concentration time course, the oral uptake rate constant (K1C) was reduced from a value of 2 to 0.51 L/h/kg$^{-0.25}$, obtained by optimization. The revised model accurately reproduced the serum kinetics of d_6-BPA [MRD, 1.8 (1.3–2.4); AFE, 1.5 (1.0–1.9)] (Fig. 7A), and tracked the time courses of serum d_6-BPAG [MRD, 2.0 (1.7–3.2); AFE, 1.4 (1.2–2.2)] (Fig. 7B) and d6-BPAS concentrations [MRD, 2.3 (1.6–3.4); AFE, 1.7 (1.0–3.3)] (Fig. 7C). Simulations of cumulative excretion of total d6-BPA in urine were also in line with collected data (Fig. 7D), with MRD of 2.7 (1.6–6.4) and AFE of 1.5 (1.1–2.0). Model predictions of serum concentration profiles of d_6-BPA, d_6-BPAG, and d_6-BPAS, as well

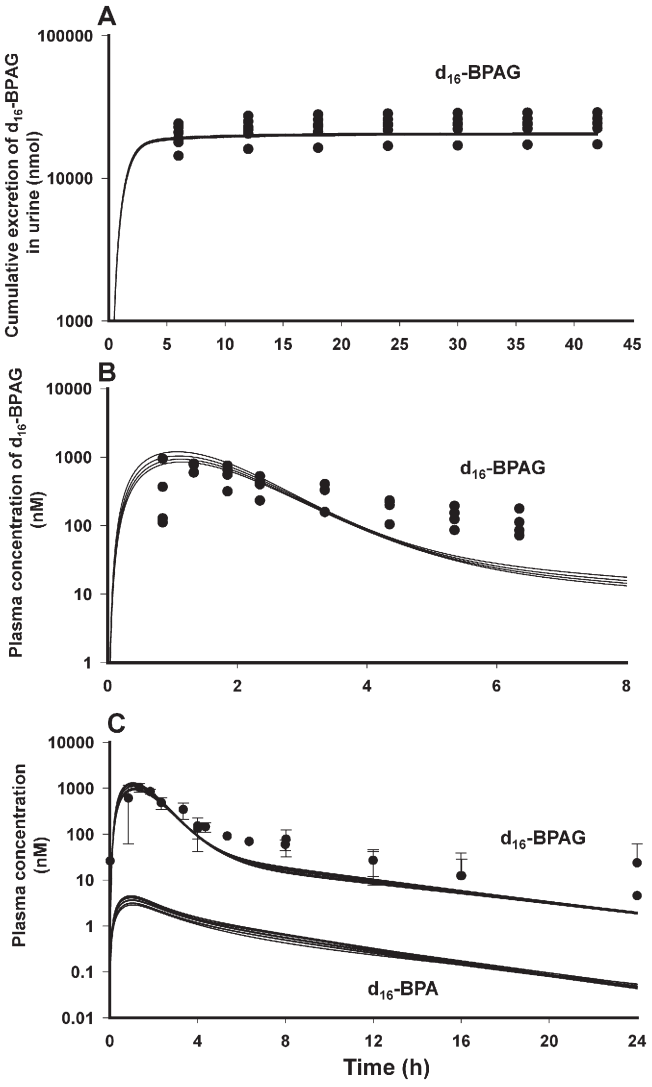

Fig. 4. Urinary excretion and concentration–time profiles after oral dosing of adult humans with 5 mg d_{16}-BPA (Völkel et al., 2002). A: Simulated (solid lines) and observed (●) individual cumulative excretion of d_{14}-BPAG in urine (n = 6); B: simulated (solid lines) and observed (●) individual plasma d_{14}-BPAG concentrations (n = 4); C: simulated individual (solid lines) and observed male and female (mean ± SD) plasma d_{14}-BPAG concentrations (n = 9) as well as simulated individual plasma d_{14}-BPA concentrations.

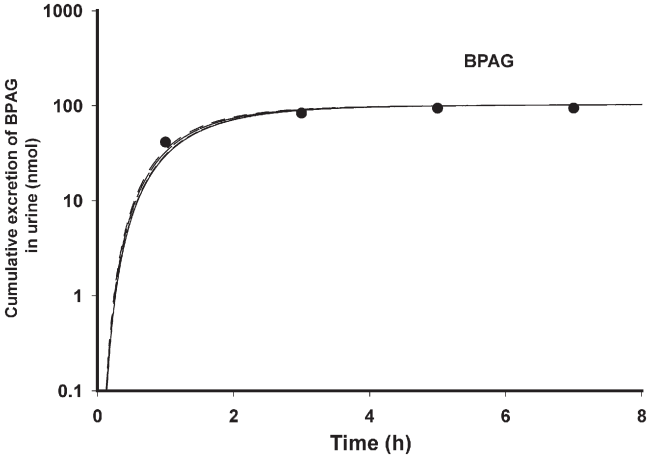

Fig. 5. Urinary excretion profiles after oral dosing of adult humans (n = 6) with 25 μg BPA (Volkel et al., 2005). Solid lines depict individual simulations and closed circles (●) represent mean values of observations of cumulative excretion of BPAG in urine.

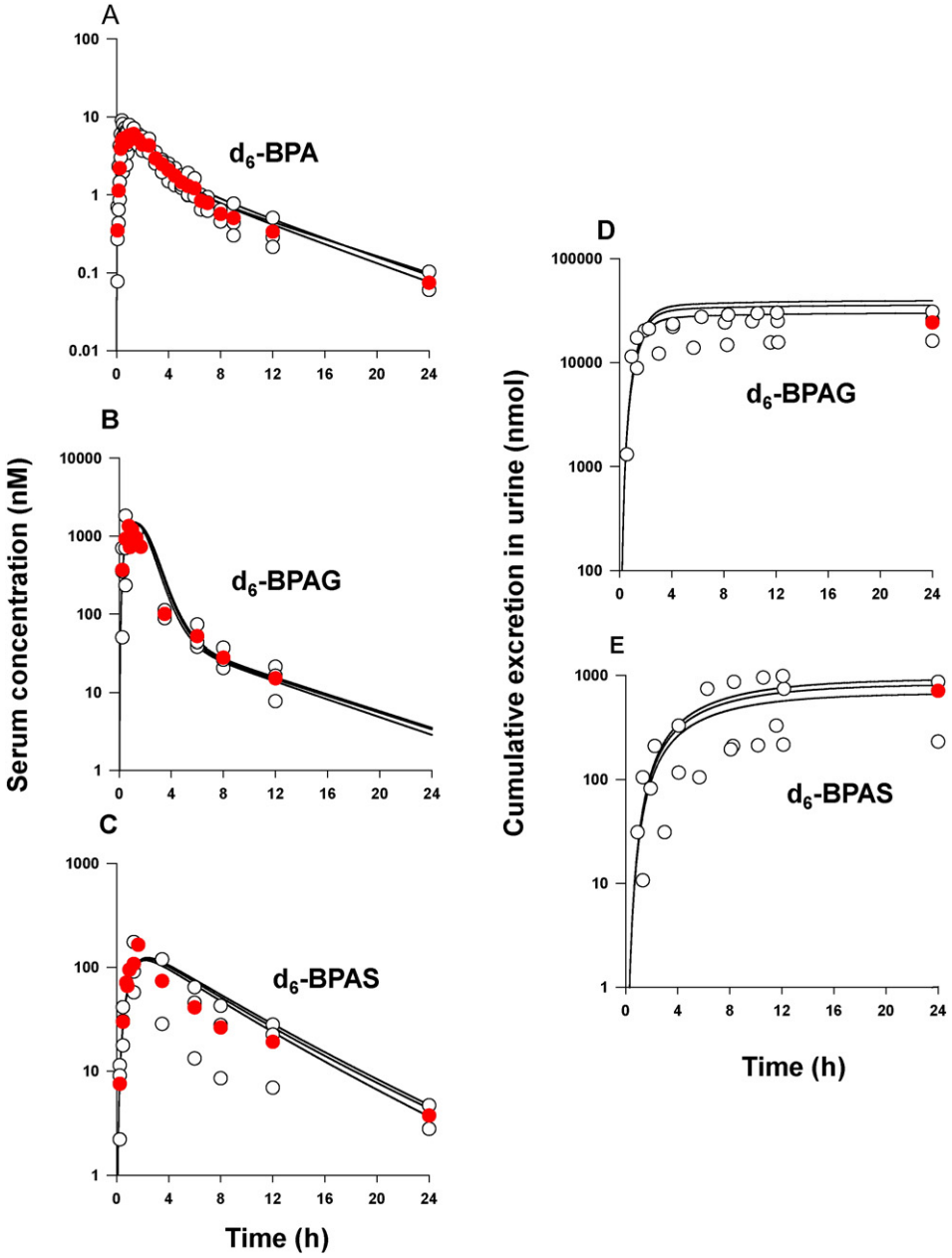

Fig. 6. Concentration–time (left panel) and urinary excretion (right panel) profiles after oral dosing of adult humans (n = 3) with 100 μg/kg d_6-BPA (Thayer et al., 2015). A: Simulated individual (solid lines) and observed individual (○) and mean (●) serum d_6-BPA concentrations; B: simulated individual (solid lines) and observed individual (○) and mean (●) serum d_6-BPAG concentrations; C: simulated individual (solid lines) and observed individual (○) and mean (●) serum d_6-BPAS concentrations; D: simulated individual (solid lines) and observed individual (○) and mean (●) cumulative excretion of d_6-BPAG in urine; E: simulated individual (solid lines) and observed individual (○) and mean (●) cumulative excretion of d_6-BPAS in urine.

as cumulative urinary excretion of total d_6-BPA for each individual are provided in Supplementary data (Fig. S2).

3.3. Sensitivity analysis

Sensitivity analysis indicated that model predicted serum d_6-BPA concentrations over a period of 24 h in adult humans after oral dosing of 100 μg/kg d_6-BPA were sensitive to model parameters as listed in Table 5, for which the calculated maximum absolute value of NSC was greater than 0.1. Also, parameters describing cardiac output (QCC), blood flow to rapidly (QRC) and slowly perfused tissues (QSC), hepatic glucuronidation (Kmliver, VmaxliverC), gastric emptying (GEC), oral uptake (K1C), glucuronidation in the GI tract (VmaxgutC), and the percent of BPAG in the liver taken up into the systemic circulation (MET) were identified to have more apparent impact on model predicted serum d_6-BPA concentration time course (with maximum absolute NSC values greater than 1). Also, among these sensitive parameters, the volume of the liver (VliverC) and partition coefficient of BPA for the liver (Pliver) impacted BPA serum concentration profiles only for the very early time points (within 5 min after dosing), and metabolic constants describing hepatic sulfation of BPA (VmaxliversC and Kmlivers) altered BPA serum concentrations only for the last few minutes, while the rest of these sensitive parameters impacted BPA serum concentrations over a wider time range (Supplementary data, Fig. S3).

3.4. Assessment of human exposure to BPA

To represent maximal exposure, the oral uptake constant (K1C, 2 L/$h/kg^{-0.25}$) determined based on the cookie data (Thayer et al., 2015),

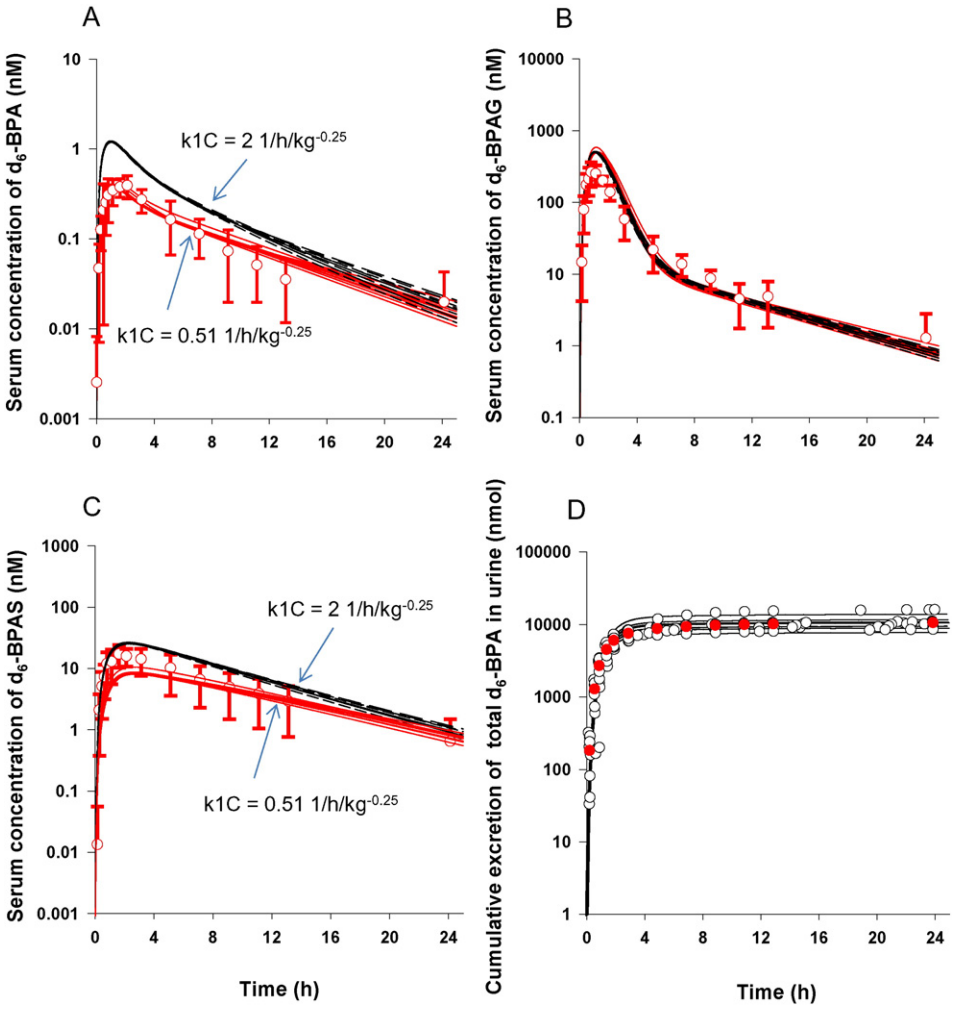

Fig. 7. Concentration–time and urinary excretion profiles after oral dosing of adult humans (n = 10) with 30 μg/kg d_6-BPA (Teeguarden et al., 2015). A: Simulated individual (lines) and observed (mean ± SD) serum d_6-BPA concentrations; B: simulated individual (lines) and observed (mean ± SD) serum d_6-BPAG concentrations; C: simulated individual (lines) and observed (mean ± SD) serum d_6-BPAS concentrations; D: simulated individual (lines) and observed individual (○) and mean (●) cumulative excretion of total d_6-BPA in urine. Monochrome discontinuous lines depict model predictions with the calibrated human model based on cookie data (Thayer et al., 2015) and red solid lines depict model predictions with the revised model based on the soup data (Teeguarden et al., 2015), i.e. oral uptake constant (K1C) reduced from 2 L/h/kg$^{-0.25}$ to 0.51 L/h/kg$^{-0.25}$. Model predictions of serum d_6-BPAG concentration time course and cumulative excretion of d_6-BPAG in urine using the calibrated model and the revised model were largely overlapped.

instead of the lesser one (0.51 L/h/kg$^{-0.25}$) derived from the soup data (Teeguarden et al., 2015), was used herein for the application of the current human BPA PBPK model for the assessment of human exposure to BPA.

Monte Carlo simulations were conducted to evaluate the inter-individual variability of model predicted internal dose metrics (C_{max} and daily AUC) of serum unconjugated BPA at steady state in the general U.S. population aged 20 years and over, with probabilistic distributions for physiological and chemical-specific model parameters derived from the literature. Fig. 8 shows the distributions of serum peak levels (C_{max}) and daily AUC of BPA at steady state associated with estimated daily oral intake of BPA for adult humans (0.2–0.5 μg/kg/day, mean-90th percentile) by U.S. FDA (FDA, 2014b) and the aggregative exposure of BPA estimated based on NHANES BPA biomonitoring data (0.05–0.27 μg/kg BW/day (median-95th percentile) (Lakind and Naiman, 2008). In general, 95% of predicted human viability in the internal dose metrics of BPA (C_{max} and daily AUC) falls within an order of magnitude (Table 6). The predicted peak serum BPA levels were in the range of pM, consistent with that calculated previously using multiple empirical approaches (Teeguarden et al., 2013).

Table 5
Sensitive model parameters. Parameters with absolute NSC values greater than 1 are highlighted in bold.

Physiological parameters	BW, **QCC**, QLiverC, QFatC, **QRC**, **QSC**, VliverC, VfatC, VRC, VSC
Partition coefficients	Pfat, Prich, Pslow, Pliver
Chemical specific model parameters	**Kmliver**, **VmaxliverC**, Kmlivers, VmaxliversC, **GEC**, **K1C**, KmgutC, **VmaxgutC**, **MET**, Kenterobpa1C, EHRrateC

4. Discussion

In the present study, the previously developed PBPK model for BPA in rhesus monkeys (Fisher et al., 2011) was modified to characterize the pharmacokinetic behaviors of BPA and its conjugates in adult humans after oral administration of BPA. New pharmacokinetic data sets used for model calibration and evaluation encompass serum concentration and urinary excretion profiles collected in adult humans following a single oral dose of d_6-BPA, where serum d_6-BPA concentrations were measured for the first time (Teeguarden et al., 2015; Thayer et al., 2015). These kinetic data sets, along with in vitro studies on BPA metabolism in the liver and the small intestine (Coughlin et al., 2012; Kurebayashi et al., 2010; Trdan Lusin et al., 2012), provide direct empirical evidence for the determination of BPA model parameters. Compared with existing human PBPK models, where systemic clearance of BPA was either set to represent the "worst-case scenario" (Edginton

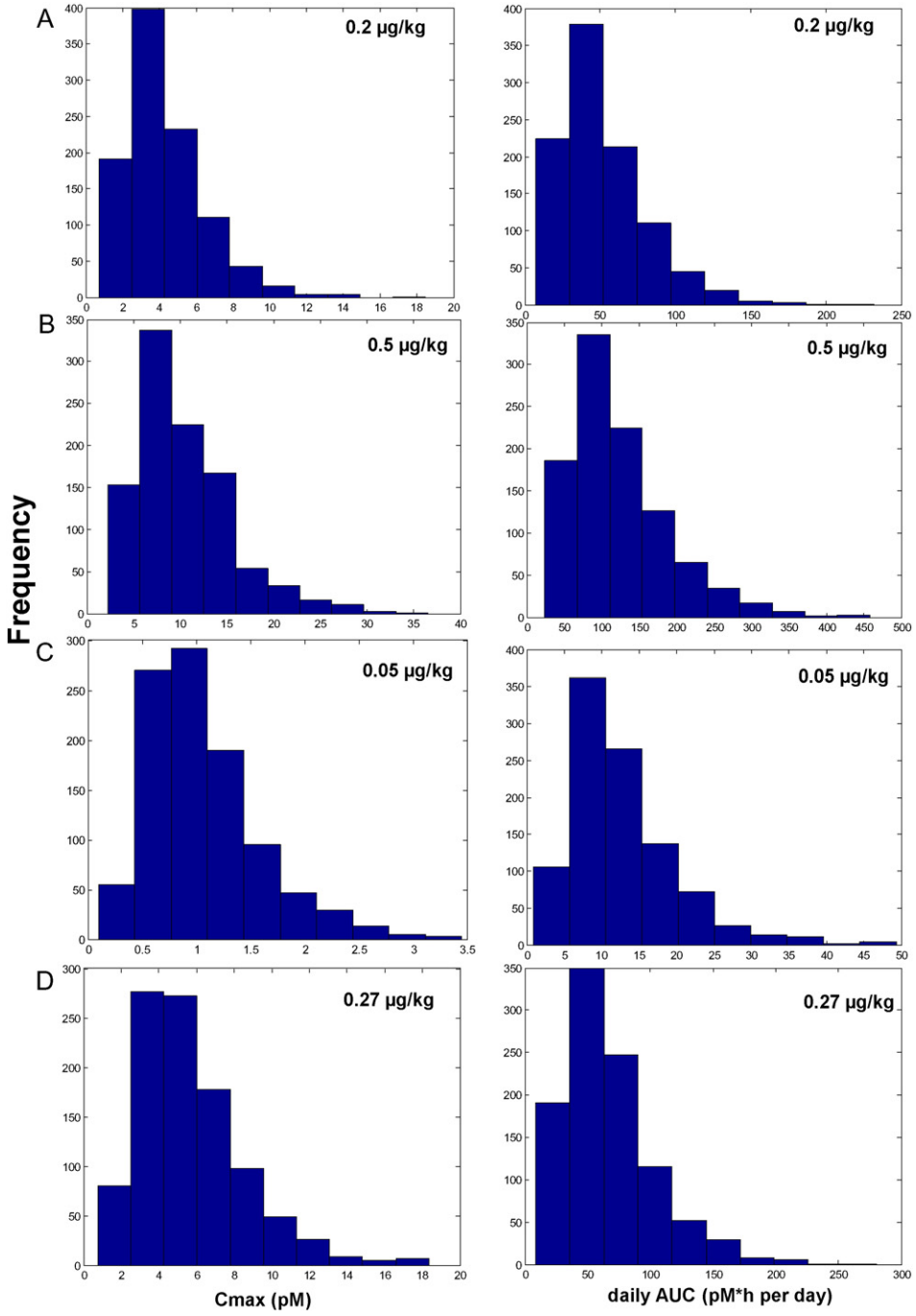

Fig. 8. Monte Carlo simulations of inter-individual variability for the general U.S. population. Distribution of model predicted peak serum levels (C_{max}) and daily area under the concentration time curve (AUC) for BPA at steady state in the general U.S. population under different exposure scenarios: A, estimated daily dietary intake of BPA at 0.2 μg/kg (mean) (FDA, 2014b); B, estimated daily dietary intake of BPA at 0.5 μg/kg (90th percentile) (FDA, 2014b); C, estimated aggregate daily total exposure of BPA at 0.05 μg/kg (median) (Lakind and Naiman, 2008); D, estimated aggregate daily total exposure of BPA at 0.27 μg/kg (95th percentile) (Lakind and Naiman, 2008).

and Ritter, 2009), based on IVIVE (Mielke and Gundert-Remy, 2009, 2012; Partosch et al., 2013), or scaled from monkey (Fisher et al., 2011) and rat (Teeguarden et al., 2005) models, the current model minimized uncertainties in BPA model parameter determination with the availability of empirical human experimental data. Therefore, the current model would be better for human exposure assessment to reduce uncertainties incurred during extrapolation across doses and species. However, due to the absence of knowledge on the exact disposition of BPA and its metabolites in the body, for example, measurements of portal vs systemic concentrations of BPA, understanding of the kinetics of BPA and its metabolites in the liver and the GI tract, some of the predictions made using our model are non-identifiable and only laboratory animal data are available.

In accordance with the original monkey model (Fisher et al., 2011), first pass metabolism (glucuronidation) of BPA in the small intestine was introduced in the current model to account for the relatively low levels of systemic d_6-BPA and rapid appearance of high levels of d_6-BPAG in serum after oral administration of d_6-BPA (Teeguarden et al., 2015; Thayer et al., 2015). Glucuronidation of BPA in the gastrointestinal (GI) tract has been documented with human intestinal microsomes (Mazur et al., 2010; Trdan Lusin et al., 2012) and human intestinal cell line (Audebert et al., 2011). The recalibrated human PBPK model for

Table 6
Predicted percentiles of the distribution of serum BPA dose metrics in adult humans.

Exposure levels (μg/kg/day)	Percentiles of serum peak levels (C_{max}, pM)								
	2.5	5	15	25	50	75	85	95	97.5
Estimated daily dietary intake (FDA, 2014b)									
0.2 (mean)	1.4	1.7	2.3	2.7	3.9	5.5	6.4	8.6	9.8
0.5 (90th percentile)	3.6	4.1	5.6	6.7	9.2	13.1	15	20.9	23.7
Estimated aggregate daily total exposure (Lakind and Naiman, 2008)									
0.05 (median)	0.35	0.42	0.58	0.69	0.95	1.33	1.58	2.14	2.40
0.27 (95th percentile)	1.9	2.2	3	3.6	5.2	7.2	8.4	11.2	12.6
Exposure levels (μg/kg/day)	Percentiles of daily AUC (pM∗h per day)								
	2.5	5	15	25	50	75	85	95	97.5
Estimated daily dietary intake (FDA, 2014b)									
0.2 (mean)	14.6	17.5	25.4	30.6	44.4	64.8	79.1	105.4	124.9
0.5 (90th percentile)	35.1	43.8	62	73	107.8	155.2	186.3	253.4	287.2
Estimated aggregate daily total exposure (Lakind and Naiman, 2008)									
0.05 (median)	3.6	4.3	6.4	7.6	10.9	15.9	19.2	26.6	31.2
0.27 (95th percentile)	19	23.4	32.9	40.6	59.4	86	102	140.2	160.3

BPA predicted that in adult humans approximately 70% of orally dosed d_6-BPA is subject to glucuronidation in the small intestine, which is somewhat less than that (90%) predicted in adult monkeys (Fisher et al., 2011). Of note, the fitting of the BPAG absorption was affected by the percent biliary excretion and BPA glucuronidation rate, that is optimization of a first order absorption rate using BPAG concentrations as the outcome metric is greatly dependent on other factors.

With the availability of serum concentration and urinary excretion-time profiles of d_6-BPAG and d_6-BPAS in adult humans following a single oral dose of 100 μg/kg d_6-BPA, the kinetic behavior of BPAG and BPAS, instead of total BPA conjugates as described in the original monkey model (Fisher et al., 2011), were characterized in the current model. Coupled with in vitro studies on BPA conjugation using human liver microsomes (Coughlin et al., 2012) and cryopreserved hepatocytes (Kurebayashi et al., 2010), hepatic glucuronidation and sulfation of BPA were described with Michaelis–Menten equations. Model simulations suggested that the majority (93%) of oral BPA taken up into the liver undergoes glucuronidation, whereas only a small portion (7%) is subject to sulfation. As a caveat, evidence for the presence of diconjugated forms of BPA in human serum and urine (12–15%) was observed in the most recent human studies (Thayer et al., 2015; Teeguarden et al., 2015). The volume of distribution for BPAG and BPAS in this paper is apparent volume of distribution with no physiological meaning. The processing of the conjugates appears to be complex and involves both the liver and gastrointestinal tract. Several model parameters in this model, describing GI tract metabolism and EHR, are not identifiable because of the lack of data. In the paper of Edginton and Ritter (2009), the predicted distribution volume of BPAG (0.43 L/kg) is close to total body water volume (0.6 L/kg) in adult humans (Davies and Morris, 1993).

An issue arose when we attempted to describe the kinetic behavior of serum d_6-BPAG, which required an assumption to account for decreased systemic clearance of d_6-BPAG at later time points. BPAG is identified as a potential human MRP3 substrate (Mazur et al., 2012). Weak expression of MRP3 has been observed on the basolateral membranes of human kidney cells (Hilgendorf et al., 2007) and tissues (Scheffer et al., 2002). However, attempts to describe the time course of serum d_6-BPAG concentration data with the assumption of renal reabsorption were not successful (simulations not shown). Based on the previous BPA PBPK model developed by Teeguarden et al. (2005), we hypothesized that a small fraction (10%) of BPAG in the liver derived from the small intestine and the liver undergoes biliary excretion and subsequent EHR. Such an assumption was necessary to describe the lingering of serum d_6-BPAG levels, as well as serum d_6-BPA levels, at later time points. Despite the lack of direct evidence to support this hypothesis, biliary excretion and enterohepatic recirculation have been reported in humans for many other glucuronidated compounds (Caldwell and Greenberger, 1971; Herman et al., 1989; Hiller et al., 1999; Miller, 1984; Pedersen and Miller, 1980; Rollins and Klaassen, 1979).

Similar to what has been suggested for monkeys in the original monkey model by Fisher et al. (2011), the exact processes controlling the complex kinetic behavior of BPAG in humans remain uncertain. The current assumption that BPAG undergoes biliary excretion and subsequent EHR may be inappropriate, given that BPAG does not appear to be a substrate for human MRP2, MDR1, and BCRP (Mazur et al., 2012), which are major hepatic canalicular transporters responsible for biliary excretion of chemicals (Morrissey et al., 2012). Also, since gall bladder emptying in humans is not a continuous process but occurs at meal times only, the assumption of biliary excretion along with enterohepatic recirculation, in theory, could result in bumps in the BPA curve. An alternative explanation for the decreased systemic clearance of BPAG at later time points could be that BPAG in the intestinal mucosa is transported back into intestine by transporters, deconjugated by bacteria, and reabsorbed into portal vein as BPA. In addition, the slower terminal phase of BPAG could be due to the larger volume of distribution, thus slowing the terminal phase.

When the recalibrated adult human BPA PBPK model was evaluated against other kinetic data with BPA, where the time course of serum concentration and urinary excretion profiles of BPAG were collected in adult humans dosed with 5 mg d_{16}-BPA in a hard gelatin capsule (Völkel et al., 2002) and 25 μg BPA in 50 ml of water (Volkel et al., 2005), model predictions were in general in line with experimental observations (Fig. 4 and Fig. 5), suggesting the robustness of the current model with regards to the description of the kinetic behavior of BPAG. However, attempts to describe the time courses of serum d_6-BPA and d_6-BPAS concentrations in adult humans dosed with d_6-BPA in soup (Teeguarden et al., 2015) using the current model calibrated with the cookie data (Thayer et al., 2015) were not successful, and observations fell outside bounds expected when inter-individual variability was considered (data not shown). The fasting conditions and dosing vehicles used in the study of Teeguarden et al. (2015) differ from the cookie study (Thayer et al., 2015), which could impact BPA disposition, in particular during the absorption phase. To achieve better agreement with serum d_6-BPA and d_6-BPAS concentration profiles collected in the soup study (Teeguarden et al., 2015), the oral uptake rate constant (K1C) was decreased from 2 $kg^{0.25}$/h to 0.51 $kg^{0.25}$/h, implying that oral uptake of BPA may differ depending on the oral dosing vehicles (cookies versus soup) and/or fasting conditions (fed versus fasted state). In addition, the temperature and the composition of the soup as well as the time to take it may also affect vehicle effect on BPA absorption.

Parameters describing oral uptake of BPA (K1C) and glucuronidation of BPA in the small intestine (KmgutC, VmaxgutC) were demonstrated to exhibit substantial impact on model-predicted serum BPA levels, in particular during the absorption phase (Table 5 and Fig. S3). Impact of dosing vehicles on the disposition of BPA, e.g. gastric emptying time, transient time in the small intestine, as well as metabolism of BPA in the GI tract, was also proposed in the monkey BPA PBPK model (Fisher et al., 2011). More studies are needed to understand fully the impact of dosing vehicles (cookies versus soup) and fasting conditions (fasting versus fed state) on BPA kinetics and to reduce the uncertainty in the estimation of BPA model parameters.

As pointed out by Teeguarden et al. (2015), a significant positive association was observed between body mass index (BMI) and $AUC_{0\rightarrow\infty}$ as indicated by linear correlation analysis. In the current human PBPK model for BPA, a linear correlation between logBMI and the fraction of body weight for fat volume (VfatC) (Jackson et al., 2002) was used to calculate body fat volume. Analysis of the individual data from the cookie study (Thayer et al., 2015) and the soup study (Teeguarden et al., 2015) suggested that the volume of body fat (Vfat) is linearly linked

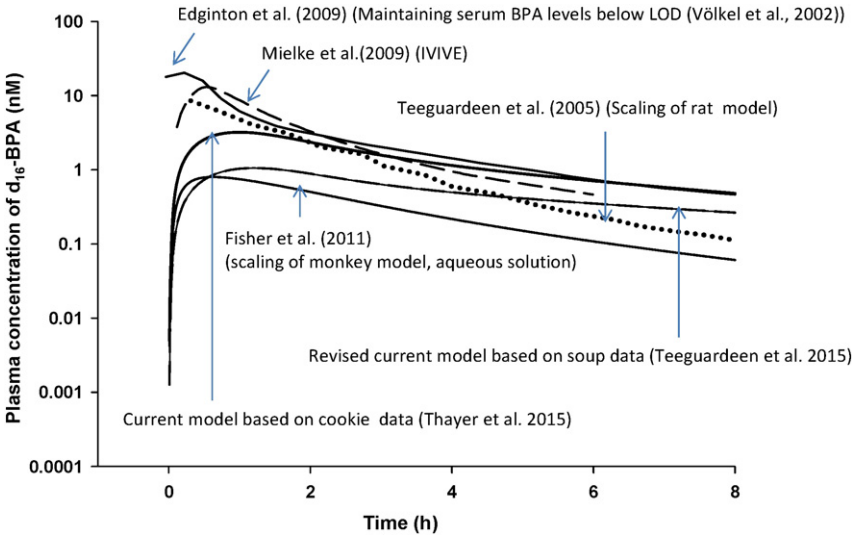

Fig. 9. Comparisons of model simulated serum d_{14}-BPA concentration time course after oral dosing of 5 mg d_{16}-BPA in hard capsules (Völkel et al., 2002) using the current model calibrated with the cookie data (Thayer et al., 2015) and the revised model based on the soup data (Teeguarden et al., 2015) as well as existing human BPA PBPK models (Edginton and Ritter, 2009; Fisher et al., 2011; Mielke and Gundert-Remy, 2009; Teeguarden et al., 2005). Simulations using the existing human BPA PBPK models were obtained by digitization from (Edginton and Ritter, 2009; Fisher et al., 2011; Mielke and Gundert-Remy, 2009; Teeguarden et al., 2005). LOD, limit of detection.

with BMI values, with a correlation coefficient of 0.96 (N = 24). Therefore, the positive association observed between BMI and $AUC_{0 \rightarrow \infty}$ (Teeguarden et al., 2015) could be in part explained by the linear correlation between BMI and the volume of fat (Vfat). As a moderate lipophilic chemical, distribution of BPA into the larger volume of fat would reduce the clearance of BPA, thus yielding the increased $AUC_{0 \rightarrow \infty}$.

Plasma concentration and cumulative urinary excretion data of d_{14}-BPAG in adult humans administered with a single oral dose of 5 mg d_{16}-BPA (Völkel et al., 2002) were the primary data set used for model development in previous human BPA PBPK models (Edginton and Ritter, 2009; Fisher et al., 2011; Mielke and Gundert-Remy, 2009; Teeguarden et al., 2005), where serum d_{14}-BPA concentration time course data were not available but simulated in these models. To compare model performance of the current model with the existing human BPA PBPK models, simulations of plasma d_{14}-BPA concentration time course (Völkel et al., 2002) with these models were evaluated. As shown in Fig. 9, the current model calibrated with the cookie data (Thayer et al., 2015) and the revised model based on soup data (Teeguarden et al., 2015), together with the original monkey model (Fisher et al., 2011), predicted relatively lower peak levels of d_{14}-BPA in plasma compared with the other models (Edginton and Ritter, 2009; Mielke and Gundert-Remy, 2009; Teeguarden et al., 2005). Such dissimilarity suggests the impact of considering first pass metabolism of BPA in the small intestine on model predictions. Also, model predicted peak plasma d_6-BPA levels derived from Teeguarden et al. (2015) differ from those derived from Thayer et al. (2015) and Fisher et al. (2011), emphasizing the impact of dosing vehicles and fasting on the absorption phase of BPA.

In this study, the recalibrated human BPA PBPK model was used to estimate the inter-individual variability of internal dose metrics of BPA for the general population based on the estimated daily intake of BPA in the United States (FDA, 2014b; Lakind and Naiman, 2008). Model predicted peak serum BPA levels fell within the range of pM, with 95% of human variability ranged within an order of magnitude, suggesting that an uncertainty factor of less than 10 would be reasonable to account for the inter-individual variability in pharmacokinetics. Also, model predicted internal dose levels of BPA were consistent with those calculated using multiple empirical approaches (Teeguarden et al., 2013), and raised questions concerning the plausibility of a small subset of high serum BPA levels reported in literature.

Supplementary data to this article can be found online at http://dx.doi.org/10.1016/j.taap.2015.10.016.

Transparency document

The Transparency document associated with this article can be found, in the online version.

Acknowledgment

This work was supported by the U.S. Food and Drug Administration/National Center for the Toxicological Research. The authors gratefully acknowledge the help with statistics from Dr. Nysia George, and the critical review of this manuscript by Drs. Barry Delclos, Jia-Long Fang, Jason Aungst, and Frederick A. Beland. The manuscript does not necessarily reflect the views of the U.S. Food and Drug Administration. The authors have no conflict of interest.

References

Audebert, M., Dolo, L., Perdu, E., Cravedi, J.P., Zalko, D., 2011. Use of the gammah2ax assay for assessing the genotoxicity of bisphenol A and bisphenol F in human cell lines. Arch. Toxicol. 85, 1463–1473.

Bartels, M., Rick, D., Lowe, E., Loizou, G., Price, P., Spendiff, M., et al., 2012. Development of PK- and PBPK-based modeling tools for derivation of biomonitoring guidance values. Comput. Methods Prog. Biomed. 108, 773–788.

Barter, Z.E., Bayliss, M.K., Beaune, P.H., Boobis, A.R., Carlile, D.J., Edwards, R.J., et al., 2007. Scaling factors for the extrapolation of in vivo metabolic drug clearance from in vitro data: reaching a consensus on values of human microsomal protein and hepatocellularity per gram of liver. Curr. Drug Metab. 8, 33–45.

Biedermann, S., Tschudin, P., Grob, K., 2010. Transfer of bisphenol A from thermal printer paper to the skin. Anal. Bioanal. Chem. 398, 571–576.

Brown, R.P., Delp, M.D., Lindstedt, S.L., Rhomberg, L.R., Beliles, R.P., 1997. Physiological parameter values for physiologically based pharmacokinetic models. Toxicol. Ind. Health. 13, 407–484.

Calafat, A.M., Ye, X., Wong, L.Y., Reidy, J.A., Needham, L.L., 2008. Exposure of the U.S. population to bisphenol A and 4-tertiary-octylphenol: 2003–2004. Environ. Health Perspect. 116, 39–44.

Caldwell, J.H., Greenberger, N.J., 1971. Interruption of the enterohepatic circulation of digitoxin by cholestyramine. I. Protection against lethal digitoxin intoxication. J. Clin. Invest. 50, 2626–2637.

CDC. 2014. Fourth national report on human exposure to environmental chemicals. Updated tables, August, 2014. Available at http://www.Cdc.Gov/exposurereport/pdf/fourthreport_updatedtables_aug2014.Pdf. Last accessed: December 15, 2014.

Churchwell, M.I., Camacho, L., Vanlandingham, M.M., Twaddle, N.C., Sepehr, E., Delclos, K.B., et al., 2014. Comparison of life-stage-dependent internal dosimetry for bisphenol A, ethinyl estradiol, a reference estrogen, and endogenous estradiol to test an estrogenic mode of action in Sprague Dawley rats. Toxicological Sciences: an official journal of the Society of Toxicology 139, 4–20.

Clewell 3rd, H.J., Lee, T.S., Carpenter, R.L., 1994. Sensitivity of physiologically based pharmacokinetic models to variation in model parameters: methylene chloride. Risk Anal. 14, 521–531.

Clewell 3rd, H.J., Gentry, P.R., Covington, T.R., Gearhart, J.M., 2000. Development of a physiologically based pharmacokinetic model of trichloroethylene and its metabolites for use in risk assessment. Environ. Health Perspect. 108 (Suppl. 2), 283–305.

Coughlin, J.L., Thomas, P.E., Buckley, B., 2012. Inhibition of genistein glucuronidation by bisphenol A in human and rat liver microsomes. Drug Metabolism and Disposition: the biological fate of chemicals 40, 481–485.

Covington, T.R., Robinan Gentry, P., Van Landingham, C.B., Andersen, M.E., Kester, J.E., Clewell, H.J., 2007. The use of Markov chain Monte Carlo uncertainty analysis to support a public health goal for perchloroethylene. Regulatory Toxicology and Pharmacology: RTP 47, 1–18.

Davies, B., Morris, T., 1993. Physiological parameters in laboratory animals and humans. Pharm. Res. 10, 1093–1095.

Delic, J.I., Lilly, P.D., MacDonald, A.J., Loizou, G.D., 2000. The utility of PBPK in the safety assessment of chloroform and carbon tetrachloride. Regulatory Toxicology and Pharmacology: RTP 32, 144–155.

Doerge, D.R., Twaddle, N.C., Vanlandingham, M., Brown, R.P., Fisher, J.W., 2011. Distribution of bisphenol A into tissues of adult, neonatal, and fetal Sprague–Dawley rats. Toxicol. Appl. Pharmacol. 255, 261–270.

Edginton, A.N., Schmitt, W., Willmann, S., 2006. Development and evaluation of a generic physiologically based pharmacokinetic model for children. Clin. Pharmacokinet. 45, 1013–1034.

Edginton, A.N., Ritter, L., 2009. Predicting plasma concentrations of bisphenol A in children younger than 2 years of age after typical feeding schedules, using a physiologically based toxicokinetic model. Environ. Health Perspect. 117, 645–652.

EFSA. 2014. Scientific opinion on the risks to public health related to the presence of bisphenol A (BPA) in foodstuffs; question number efsa-q-2012-00423. Available at: http://www.efsa.europa.eu/en/consultationsclosed/call/140117.pdf. Last accessed: December 15, 2014.

Elsby, R., Maggs, J.L., Ashby, J., Park, B.K., 2001. Comparison of the modulatory effects of human and rat liver microsomal metabolism on the estrogenicity of bisphenol A: implications for extrapolation to humans. The Journal of Pharmacology and Experimental Therapeutics 297, 103–113.

FDA. 2014a. Bisphenol A (BPA): use in food contact application. http://www.fda.gov/NewsEvents/PublicHealthFocus/ucm064437.htm. Last assessed January 11, 2015.

FDA. 2014b. Memorandum: 2014 updated safety assessment of bisphenol A (BPA) for use in food contact applications. Available at http://www.fda.gov/downloads/newsevents/publichealthfocus/ucm424266.pdf. Last assessed: December 15, 2014.

Fisher, J.W., Twaddle, N.C., Vanlandingham, M., Doerge, D.R., 2011. Pharmacokinetic modeling: prediction and evaluation of route dependent dosimetry of bisphenol A in monkeys with extrapolation to humans. Toxicol. Appl. Pharmacol. 257, 122–136.

Geens, T., Aerts, D., Berthot, C., Bourguignon, J.P., Goeyens, L., Lecomte, P., et al., 2012. A review of dietary and non-dietary exposure to bisphenol-A. Food and Chemical Toxicology: an international journal published for the British Industrial Biological Research Association 50, 3725–3740.

Herman, R.J., Van Pham, J.D., Szakacs, C.B., 1989. Disposition of lorazepam in human beings: enterohepatic recirculation and first-pass effect. Clin. Pharmacol. Ther. 46, 18–25.

Hilgendorf, C., Ahlin, G., Seithel, A., Artursson, P., Ungell, A.L., Karlsson, J., 2007. Expression of thirty-six drug transporter genes in human intestine, liver, kidney, and organotypic cell lines. Drug Metabolism and Disposition: the biological fate of chemicals 35, 1333–1340.

Hiller, A., Nguyen, N., Strassburg, C.P., Li, Q., Jainta, H., Pechstein, B., et al., 1999. Retigabine n-glucuronidation and its potential role in enterohepatic circulation. Drug Metabolism and Disposition: the biological fate of chemicals 27, 605–612.

Ito, K., Houston, J.B., 2005. Prediction of human drug clearance from in vitro and preclinical data using physiologically based and empirical approaches. Pharm. Res. 22, 103–112.

Jackson, A.S., Stanforth, P.R., Gagnon, J., Rankinen, T., Leon, A.S., Rao, D.C., et al., 2002. The effect of sex, age and race on estimating percentage body fat from body mass index: the heritage family study. International journal of obesity and related metabolic disorders: journal of the International Association for the Study of Obesity 26, 789–796.

Kortejarvi, H., Urtti, A., Yliperttula, M., 2007. Pharmacokinetic simulation of biowaiver criteria: the effects of gastric emptying, dissolution, absorption and elimination rates. Eur. J. Pharm. Sci. 30, 155–166.

Kuester, R.K., Sipes, I.G., 2007. Prediction of metabolic clearance of bisphenol A (4,4′-dihydroxy-2,2-diphenylpropane) using cryopreserved human hepatocytes. Drug metabolism and Disposition: the biological fate of chemicals 35, 1910–1915.

Kurebayashi, H., Okudaira, K., Ohno, Y., 2010. Species difference of metabolic clearance of bisphenol A using cryopreserved hepatocytes from rats, monkeys and humans. Toxicol. Lett. 198, 210–215.

Lakind, J.S., Naiman, D.Q., 2008. Bisphenol A (BPA) daily intakes in the United States: estimates from the 2003–2004 NHANES urinary BPA data. Journal of Exposure Science & Environmental Epidemiology 18, 608–615.

LaKind, J.S., Goodman, M., Naiman, D.Q., 2012. Use of NHANES data to link chemical exposures to chronic diseases: a cautionary tale. PLoS One 7, e51086.

Lang, I.A., Galloway, T.S., Scarlett, A., Henley, W.E., Depledge, M., Wallace, R.B., et al., 2008. Association of urinary bisphenol A concentration with medical disorders and laboratory abnormalities in adults. JAMA 300, 1303–1310.

Matthews, J.B., Twomey, K., Zacharewski, T.R., 2001. In vitro and in vivo interactions of bisphenol A and its metabolite, bisphenol A glucuronide, with estrogen receptors alpha and beta. Chem. Res. Toxicol. 14, 149–157.

Mazur, C.S., Kenneke, J.F., Hess-Wilson, J.K., Lipscomb, J.C., 2010. Differences between human and rat intestinal and hepatic bisphenol A glucuronidation and the influence of alamethicin on in vitro kinetic measurements. Drug Metabolism and Disposition: the biological fate of chemicals 38, 2232–2238.

Mazur, C.S., Marchitti, S.A., Dimova, M., Kenneke, J.F., Lumen, A., Fisher, J., 2012. Human and rat ABC transporter efflux of bisphenol A and bisphenol A glucuronide: interspecies comparison and implications for pharmacokinetic assessment. Toxicological Sciences: an official journal of the Society of Toxicology 128, 317–325.

Melzer, D., Rice, N.E., Lewis, C., Henley, W.E., Galloway, T.S., 2010. Association of urinary bisphenol A concentration with heart disease: evidence from NHANES 2003/06. PLoS One 5, e8673.

Mielke, H., Gundert-Remy, U., 2009. Bisphenol A levels in blood depend on age and exposure. Toxicol. Lett. 190, 32–40.

Mielke, H., Partosch, F., Gundert-Remy, U., 2011. The contribution of dermal exposure to the internal exposure of bisphenol A in man. Toxicol. Lett. 204, 190–198.

Mielke, H., Gundert-Remy, U., 2012. Physiologically based toxicokinetic modelling as a tool to support risk assessment: three case studies. Journal of Toxicology 2012, 359471.

Miller, R., 1984. Pharmacokinetics and bioavailability of ranitidine in humans. J. Pharm. Sci. 73, 1376–1379.

Morrissey, K.M., Wen, C.C., Johns, S.J., Zhang, L., Huang, S.M., Giacomini, K.M., 2012. The UCSF-FDA transportal: a public drug transporter database. Clin. Pharmacol. Ther. 92, 545–546.

Ogden, C.L., Fryar, C.D., Carroll, M.D., Flegal, K.M., 2004. Mean Body Weight, Height, and Body Mass Index, United States 1960–2002. Advance Data from Vital and Health Statistics; no 347. National Center for Health Statistics, Hyattsville, Maryland.

Paine, M.F., Khalighi, M., Fisher, J.M., Shen, D.D., Kunze, K.L., Marsh, C.L., et al., 1997. Characterization of interintestinal and intraintestinal variations in human cyp3a-dependent metabolism. The Journal of Pharmacology and Experimental Therapeutics 283, 1552–1562.

Partosch, F., Mielke, H., Gundert-Remy, U., 2013. Functional UDP-glucuronyltransferase 2b15 polymorphism and bisphenol A concentrations in blood: results from physiologically based kinetic modelling. Arch. Toxicol. 87, 1257–1264.

Patterson, T.A., Twaddle, N.C., Roegge, C.S., Callicott, R.J., Fisher, J.W., Doerge, D.R., 2013. Concurrent determination of bisphenol A pharmacokinetics in maternal and fetal rhesus monkeys. Toxicol. Appl. Pharmacol. 267, 41–48.

Pedersen, P.V., Miller, R., 1980. Pharmacokinetics of doxycycline reabsorption. J. Pharm. Sci. 69, 204–207.

Riley, R.J., McGinnity, D.F., Austin, R.P., 2005. A unified model for predicting human hepatic, metabolic clearance from in vitro intrinsic clearance data in hepatocytes and microsomes. Drug Metabolism and Disposition: the biological fate of chemicals 33, 1304–1311.

Rollins, D.E., Klaassen, C.D., 1979. Biliary excretion of drugs in man. Clin. Pharmacokinet. 4, 368–379.

Scheffer, G.L., Kool, M., de Haas, M., de Vree, J.M., Pijnenborg, A.C., Bosman, D.K., et al., 2002. Tissue distribution and induction of human multidrug resistant protein 3. Laboratory Investigation; a journal of technical methods and pathology 82, 193–201.

Schmitt, W., 2008. General approach for the calculation of tissue to plasma partition coefficients. Toxicology In Vitro: an international journal published in association with BIBRA 22, 457–467.

Shankaran, H., Adeshina, F., Teeguarden, J.G., 2013. Physiologically-based pharmacokinetic model for fentanyl in support of the development of provisional advisory levels. Toxicol. Appl. Pharmacol. 273, 464–476.

Shimizu, M., Ohta, K., Matsumoto, Y., Fukuoka, M., Ohno, Y., Ozawa, S., 2002. Sulfation of bisphenol A abolished its estrogenicity based on proliferation and gene expression in human breast cancer mcf-7 cells. Toxicology In Vitro: an international journal published in association with BIBRA 16, 549–556.

Silver, M.K., O'Neill, M.S., Sowers, M.R., Park, S.K., 2011. Urinary bisphenol A and type-2 diabetes in U.S. adults: data from NHANES 2003–2008. PLoS One 6, e26868.

Sterner, T.R., Ruark, C.D., Covington, T.R., Yu, K.O., Gearhart, J.M., 2013. A physiologically based pharmacokinetic model for the oxime TMB-4: simulation of rodent and human data. Arch. Toxicol. 87, 661–680.

Tan, Y.M., Liao, K.H., Conolly, R.B., Blount, B.C., Mason, A.M., Clewell, H.J., 2006. Use of a physiologically based pharmacokinetic model to identify exposures consistent with human biomonitoring data for chloroform. Journal of Toxicology and Environmental Health Part A 69, 1727–1756.

Teeguarden, J., Hanson-Drury, S., Fisher, J.W., Doerge, D.R., 2013. Are typical human serum BPA concentrations measurable and sufficient to be estrogenic in the general population? Food and Chemical Toxicology: an international journal published for the British Industrial Biological Research Association 62, 949–963.

Teeguarden, J.G., Waechter Jr., J.M., Clewell 3rd, H.J., Covington, T.R., Barton, H.A., 2005. Evaluation of oral and intravenous route pharmacokinetics, plasma protein binding, and uterine tissue dose metrics of bisphenol A: a physiologically based pharmacokinetic approach. Toxicological Sciences: an official journal of the Society of Toxicology 85, 823–838.

Teeguarden, J.G., Calafat, A.M., Ye, X., Doerge, D.R., Churchwell, M.I., Gunawan, R., et al., 2011. Twenty-four hour human urine and serum profiles of bisphenol A during high-dietary exposure. Toxicological Sciences: an official journal of the Society of Toxicology 123, 48–57.

Teeguarden, J.G., Twaddle, N., Churchwell, M.I., Yang, X., Fisher, J.W., Seryak, L.M., et al., 2015. 24-hour human urine and serum profiles of bisphenol A: evidence against sublingual absorption following ingestion in soup. Toxicol. Appl. Pharmacol. 288 (2), 131–142.

Thayer, K.A., Doerge, D.R., Hunt, D., Schurman, S.H., Twaddle, N.C., Churchwell, M.I., et al., 2015. Pharmacokinetics of bisphenol A in humans following a single oral administration. Environ. Int. 83, 107–115.

Trdan Lusin, T., Roskar, R., Mrhar, A., 2012. Evaluation of bisphenol A glucuronidation according to UGT1A1*28 polymorphism by a new LC–MS/MS assay. Toxicology 292, 33–41.

Twaddle, N.C., Churchwell, M.I., Vanlandingham, M., Doerge, D.R., 2010. Quantification of deuterated bisphenol A in serum, tissues, and excreta from adult Sprague–Dawley rats using liquid chromatography with tandem mass spectrometry. Rapid Communications in Mass Spectrometry: RCM 24, 3011–3020.

Vogt, W., 2014. Evaluation and optimisation of current milrinone prescribing for the treatment and prevention of low cardiac output syndrome in paediatric patients after open heart surgery using a physiology-based pharmacokinetic drug-disease model. Clin. Pharmacokinet. 53, 51–72.

Volkel, W., Bittner, N., Dekant, W., 2005. Quantitation of bisphenol A and bisphenol A glucuronide in biological samples by high performance liquid chromatography-tandem mass spectrometry. Drug Metabolism and Disposition: the biological fate of chemicals 33, 1748–1757.

Völkel, W., Colnot, T., Csanady, G.A., Filser, J.G., Dekant, W., 2002. Metabolism and kinetics of bisphenol A in humans at low doses following oral administration. Chem. Res. Toxicol. 15, 1281–1287.

WHO. 2011. Joint FAO/WHO expert meeting to review toxicological and health aspects of bisphenol A: Final report, including report of stakeholder meeting on bisphenol A, 1–5 November 2010, Ottawa, Canada. http://apps.who.int/iris/bitstream/10665/44624/1/97892141564274_eng.pdf. Last assessed: August 28, 2014.

Willhite, C.C., Ball, G.L., McLellan, C.J., 2008. Derivation of a bisphenol A oral reference dose (RfD) and drinking-water equivalent concentration. Journal of Toxicology and Environmental Health Part B, Critical reviews 11, 69–146.

Yang, X., Doerge, D.R., Fisher, J.W., 2013. Prediction and evaluation of route dependent dosimetry of bpa in rats at different life stages using a physiologically based pharmacokinetic model. Toxicol. Appl. Pharmacol. 270, 45–59.

Yu, L.X., Lipka, E., Crison, J.R., Amidon, G.L., 1996. Transport approaches to the biopharmaceutical design of oral drug delivery systems: prediction of intestinal absorption. Adv. Drug Deliv. Rev. 19, 359–376.

Zalko, D., Jacques, C., Duplan, H., Bruel, S., Perdu, E., 2011. Viable skin efficiently absorbs and metabolizes bisphenol A. Chemosphere 82, 424–430.